Aspects of loop quantum gravity

Alexander Nagen

23 September 2020

Submitted in partial fulfilment of the requirements for the degree of Master of Science of Imperial College London

Contents

1 Introduction

A significant outstanding problem in modern theoretical physics is to unify gravity and quantum mechanics [1] (QM) into a theory of quantum gravity [2]. Quantum gravity describes gravity and its phenomena on scales comparable to the smallest length scale, the Planck scale. A theory of quantum gravity is a framework that gives a complete quantum description of gravity. There are many theories that are candidates for quantum gravity [2]. The approaches of these candidates are diverse and often rely on additional assumptions such as new particles or extra dimensions. However, none of the candidates have been generally accepted. This is mainly because there is little experimental data available to test them and the data that exists does not support any of the assumptions that they make. As a result, the theory of quantum gravity that best describes our universe is not yet known.

Today, the most widely-accepted theory of gravity is general relativity [3] (GR). GR describes gravity on large length scales and is in very good agreement with experiments [3]. In GR, gravity arises as a property of spacetime. However, GR is a classical theory and, hence, cannot be a candidate for quantum gravity. This is because, contrary to the expectations of QM, GR makes no attempt to quantise spacetime or the gravitational field [2]. Also, GR predicts the existence of black hole and cosmological singularities at which it breaks down [3]. These singularities might not be physical and spacetime and gravity near them are expected to be described according to QM [3]. It may be difficult to see how GR and QM can be unified as they have seemingly irreconcilable differences.

GR unifies space and time via spacetime whereas QM treats space and time independently [2]. Also, GR is deterministic while QM is probabilistic [2].

Despite their differences, GR and QM are not incompatible [4]. At length scales where GR is valid, a unification of GR and QM is possible [4]. The resulting theory predicts the existence of a particle that carries the gravitational force, the graviton. The theory breaks down at small scales, particularly when trying to describe certain graviton scattering processes [5]. At this point, it might be expected that a full understanding of gravity, including on small to Planck scales and near classical singularities, is gained from a fully-fledged theory of quantum gravity [4].

One possible candidate for quantum gravity [2] is loop quantum gravity (LQG). LQG is a theory that fundamentally describes spacetime as being quantised. LQG is a non-perturbative theory; i.e, its construction does not depend on approximate methods. Also, LQG is background-independent; i.e, it does not assume any background spacetime. A consequence of this is that all physical predictions of LQG are background-independent.

GR has multiple formulations [6]. Each formulation expresses the physics of GR in a different way. A common formulation of GR is the metric formulation; this expresses GR in terms of the metric, Christoffel symbols, Ricci tensor etc. of spacetime. The equations of motion of spacetime in the metric formulation are the Einstein field equations. However, some of these are actually constraints on spacetime like how a particle on a ring is constrained to move on the ring. The classical theory of interest to LQG theorists is a formulation of GR in terms of a

theory that usually describes the W and Z bosons from the standard model [7] (SM). The constraints in the metric formulation carry over to this formulation and govern the physics of GR in the classical theory [6]. The re-formulation of GR is very useful as it relates GR with frameworks that are more familiar. It also makes GR easier to quantise. LQG results from quantising the classical theory [2, 6].

LQG has two formulations: canonical and covariant. The canonical formulation describes LQG in terms of spin networks. A spin network looks like a closed Feynman diagram; that is, a Feynman diagram with all its lines joined to each other. Each part of a spin network is labelled by a quantum number [2] as the energy levels of an atom are. We call a set of spin networks that which can be obtained from a given spin network by stretching it, squashing it and moving it around. A set of spin networks can be considered a state of space [2]. Superposing all possible spatial states in a certain way gives a certain configuration of space [2] like how a state of a quantum system is a superposition of all of its eigenstates. By this description, space is quantised; i.e, it consists of discrete elements like how matter consists of atoms. The canonical description of the dynamics of LQG is governed by a Hamiltonian operator [2]; this implements one of the constraints in the classical theory.

On the other hand, the covariant formulation encodes the dynamics of LQG in terms of spin foams. A spin foam governs a possible evolution between sets of spin networks [2]. The author imagines the evolution in the following way. Take a film and disassemble it into its constituent frames. Next, replace each frame

with a set of spin networks. The resulting "film" is a spin foam, although the evolution of "frames" does not happen in time. A spin foam can be considered a state of spacetime due to its interpretation as an evolution between states of space. A configuration of quantum spacetime is a certain superposition of spin foams.

A remarkable prediction of LQG is that area and volume are quantised so have discrete sets of values. In particular, there is a smallest unit of area and volume on the order of the Planck scale and below which quantum spacetime breaks down. These predictions can be attributed to the quantisation of space in LQG. The set of values of area and volume are physical predictions of LQG [2]. The quantum numbers of spin networks can be considered "good quantum numbers" [8] for area and volume [2]. Hence, area and volume can be simultaneously assigned to spin networks and their sets. This means that space in LQG has quantised area and volume.

LQG also allows for the addition of fermions, the gluon and the Higgs boson from the SM [2, 6]. The combined theory treats spacetime and matter on the same level by quantising them both. The theories of LQG with and without matter are similar [2]; in particular, canonical LQG with matter is described in terms of spin networks. Sets of spin networks have extra quantum numbers for numbers of particles. This gives rise to an interpretation that particles are localised on states of space [2].

The application of LQG to cosmological models has resulted in loop quantum cosmology [9] (LQC). LQC predicts that the big bang singularity at the

beginning of the universe does not happen. Instead, the universe begins with a big bounce, where it expands inwards then outwards [10], followed by a period of inflation. In addition, the universal big crunch does not occur in LQC. For references on these predictions, see [11, 12]. Also, LQC quantises the scale factor and cosmic time [2]. As the scale factor becomes large, LQC approaches classical cosmology as governed by the Friedmann equations [2]. As LQG does, LQC has both a canonical formulation [9] and a covariant formulation named "spin foam cosmology" [13] (; see [14] and references therein as well).

LQG has applications to black holes and their singularities. It is known that black holes have entropy [15, 16] analogous to a classical thermodynamical system. This entropy can be computed in LQG. Furthermore, Hawking showed [16, 17] that, due to QM, a black hole emits particles in a process called Hawking radiation. Hence, a black hole has a thermodynamic temperature [16, 17]. Hawking's calculation [16, 17] used the classical assumption that the black hole spacetime is continuous. For a fully consistent treatment of Hawking radiation, it is necessary to quantise spacetime. LQG seems like an ideal framework for this. However, there is currently no explanation as to how Hawking radiation arises from LQG [18]. By using methods from LQC and perturbing black holes with quantum corrections, it is found that classical black hole singularities disappear in LQG (; see [19] for references).

One of the problems with LQG is directly testing it. This is because it is difficult to directly probe the Planck scale. Doing so would require energies that are so high that no current particle accelerator can achieve them. The phenomenol-

ogy of LQG [20] has gained considerable attention as a possible method to test LQG. LQG phenomenology [20] is an area that uses techniques from LQG to make predictions about potentially observable artefacts from physics and astrophysics. Examples of such artefacts [20] include ultra-high-energy cosmic rays, high energy gamma rays and Hawking radiation. Cosmological tests for LQC, including the alternative universal beginning, have also been proposed [21]. LQG phenomenology alleviates the experimental difficulties of LQG but perhaps not by much.

As far as the author is aware, there are no practical uses for LQG. However, the author asks the reader to not jump to the conclusion that LQG is impractical. History has demonstrated that even the most abstract of physical theories have practical applications. GR might be considered one of these theories but it led to GPS [2]. Also, special relativity, a special case of GR, led to the television and the nuclear power station [22]. QM may also be considered abstract but it led to the development of classical computers and smartphones which some people use in their everyday lives. Given these outcomes, it is entirely possible that LQG could spawn practical applications in the future. Of course, LQG could be entirely incorrect meaning that this will not happen. However, the author encourages the reader to give LQG the benefit of the doubt in this respect.

There are several reasons why LQG is of interest. LQG incorporates GR and QM into a single unified framework. Hence, LQG may be the quantum theory of gravity that is currently missing from the SM. If experiments support LQG

and it becomes generally accepted, it may bring theoretical physics closer to a unification of all fundamental forces. Also, the majority of current research is on theories of quantum gravity influenced by particle physics. Typically, these theories quantise the gravitational field but not spacetime. On the other hand, LQG does quantise spacetime and gives insight into what a quantum spacetime might look like. Hence, LQG could be considered a more fundamental approach to quantum gravity. Furthermore, LQG requires a complete re-evaluation of how spacetime is understood. In particular, where and when an event happens in spacetime must be re-considered [2]. LQG also extends understanding of spacetime beyond classical singularities that limit GR. In doing this, LQG motivates a possible re-consideration of aspects of black hole physics and how the universe began and will end. It is intriguing that LQG directly describes the smallest scales and, via LQC, indirectly describes the largest scales. For these reasons, the author believes that LQG is worthy of attention.

The purpose of this dissertation is to review aspects of LQG. The presentation will not be overly rigorous. This dissertation is structured as follows. Chapter 2 gives a review of the construction of the classical theory mentioned earlier. In chapter 3, the classical theory is quantised in the canonical formulation. Chapter 4 covers elements of the canonical quantum theory including the celebrated results that area and volume are quantised. Chapter 5 reviews the covariant formulation and spin foams. Chapter 6 reviews applications of LQG to black holes. Chapter 7 covers topics that have been approached with LQG over the past few years. Chapter 8 presents the conclusion.

In this dissertation, where we consider 4D Lorentzian spacetimes, we use the metric signature (-,+,+,+). Also, we use units where $8\pi G = \hbar = k = c = 1$.

2 Classical theory

In this section, we review the classical theory whose quantisation yields LQG. The construction of the classical theory requires the ADM and Hamiltonian formulations of GR. Hence, we will need to review these first.

2.1 The ADM / initial-value formulation of GR

We start by reviewing the ADM formalism [23] of GR. Following [6] and the abstract index notation used in [3], we consider the tensorial objects themselves, not with respect to a set of coordinates.

We consider a spacetime $\mathcal{M}$ that is globally hyperbolic [6]; i.e, there exists an arbitrary 3D space σ such that the topology of $\mathcal{M}$ is that of $\mathbb{R} \times \sigma$. The ADM formalism foliates [3] $\mathcal{M}$ into 3D spacelike Cauchy hypersurfaces $\{\Sigma_t\}$ as

$$\mathcal{M} = \bigcup_{t \in \mathbb{R}} \Sigma_t \tag{1}$$

[24]. The function $t \in \mathbb{R}$ is called the "global time function" [3]. Although spacetime has been split up, the lack of a coordinate system means that the foliation is arbitrary [6]. This preserves the diffeomorphism symmetry of the Einstein-Hilbert action and the lack of a global time parameter in GR [6, 25]. The Lorentzian structure of $\mathcal{M}$, that includes a metric $g_{\mu\nu}$ with inverse $g^{\mu\nu}$ and a Levi-Civita connection ∇_μ, induces a Riemannian structure on each Σ_t that includes a metric and a Levi-Civita connection [3]. The induced metric is

$$q_{\mu\nu} = g_{\mu\nu} + n_\mu n_\nu \tag{2}$$

where n^μ is a timelike vector field normal to Σ_t and normalised such that $n^\mu n_\mu = -1$ [25]. The inverse of $q_{\mu\nu}$ is

$$q^{\mu\nu} = g^{\mu\nu} + n^\mu n^\nu \tag{3}$$

[24, 25]. The induced connection, D_μ, acts on a tensor field $T^{\mu_1\cdots\mu_m}_{\nu_1\ldots\nu_n}$ on Σ_t such that

$$D_\rho T^{\mu_1\cdots\mu_m}_{\nu_1\ldots\nu_n} = q^{\mu_1}_{\rho_1}\ldots q^{\mu_m}_{\rho_m} q^{\sigma_1}_{\nu_1}\ldots q^{\sigma_n}_{\nu_n} q^\sigma_\rho \nabla_\sigma T^{\rho_1\cdots\rho_m}_{\sigma_1\ldots\sigma_n} \tag{4}$$

where the indices are raised and lowered by the metric on $\mathcal{M}$ [3]. The extrinsic curvature of Σ_t is encoded in the tensor

$$K_{\mu\nu} := D_\mu n_\nu = q^\rho_\mu q^\sigma_\nu \nabla_\rho n_\sigma \tag{5}$$

[25]. It can be shown [6] that $K_{\mu\nu} = K_{(\mu\nu)}$; i.e, $K_{\mu\nu}$ is a symmetric tensor.

We introduce quantities called the lapse function N and the shift vector N^μ [6]. These are such that Nn^μ is the normal vector connecting neighbouring hypersurfaces and N^μ is tangential to the hypersurfaces [3, 6]. While the set of GR variables in the metric formulation is $g_{\mu\nu}$, that in the ADM formalism is $\{q_{\mu\nu}, N, N^\mu\}$ [3]. Part of the reasoning for this is that both sets of variables contain the same number of degrees of freedom. We call $\{q_{\mu\nu}, N, N^\mu\}$ the ADM variables. It can be shown [24] that $q_{\mu\nu}$ and $K_{\mu\nu}$ satisfy the following constraints:

$$D^\nu K_{\mu\nu} - D_\mu K = 0, \tag{6}$$

$$^{(3)}R + K^2 - K_{\mu\nu}K^{\mu\nu} = 0 \tag{7}$$

where $K = K^\mu_\mu$ and $^{(3)}R$ is the Ricci scalar of Σ_t. Respectively, (6) and (7) are the momentum and Hamiltonian constraints [24]. The vacuum Einstein field

equations in terms of $g_{\mu\nu}$ are equivalent to the system of ADM equations of motion and constraints in terms of the ADM variables [24]. It can be shown [3] that GR can be stated as a well-posed initial-value formulation as follows. As t changes, the hypersurface Σ_t labelled by t changes so the metric $q_{\mu\nu}$ on Σ_t changes. We display this functional behaviour of the 3-metric that we have suppressed so far as $q_{\mu\nu}(t)$. Equivalently, we may consider $q_{\mu\nu}(t)$ as the t-dependent metric on a fixed hypersurface $\tilde{\Sigma} \in \mathcal{M}$. Hence, we may consider $q_{\mu\nu}(t)$ as a dynamical variable. The same can be said for $K_{\mu\nu}$. Further, given initial data on a hypersurface $\overline{\Sigma} \in \mathcal{M}$ consisting of its metric $q_{\mu\nu}$ and extrinsic curvature $K_{\mu\nu}$ that solve (6) and (7), $\mathcal{M}$ is completely determined by the initial data on $\overline{\Sigma}$ and solves the vacuum Einstein field equations. Different Cauchy surfaces of $\mathcal{M}$, and so different sets of initial data, can determine $\mathcal{M}$.

2.2 Hamiltonian GR

The initial value formulation of GR is like that of other areas of physics such as classical mechanics and electrodynamics. Like these areas, GR has a Hamiltonian formulation. This uses the ADM formalism and leads to the classical theory. In this sub-chapter, we review the Hamiltonian formulation of GR.

The configuration space of GR, denoted by $Met(\sigma)$ [25], is the space spanned by the ADM variables. The phase space of GR in the Hamiltonian formulation is

$$\mathcal{P} := T^*Met(\sigma) = \{\{q_{\mu\nu}, \pi^{\mu\nu}\}, \{N, \Pi\}, \{N^\mu, \Pi_\mu\}\} \tag{8}$$

; i.e, it is the cotangent bundle of $Met(\sigma)$ spanned by the ADM variables and

their conjugate momenta [25].

The Einstein-Hilbert action is

$$S = \frac{1}{2}\int_{\mathcal{M}} R\sqrt{-g}\; d^4x \tag{9}$$

where R is the Ricci scalar of $\mathcal{M}$. First, we express S in terms of the ADM variables. Following [6], we pull all quantities back to σ from Σ_t to do this. It can be shown [3] that

$$R =^{(3)} R + K_{ab}K^{ab} - K^2 \tag{10}$$

and

$$\sqrt{-g} = |N|\sqrt{q} \tag{11}$$

where $g = |g_{ab}|$ and $q = |q_{ab}|$. Having done this, we can re-cast (9) as

$$S = \frac{1}{2}\int_{-\infty}^{\infty}\int_{\sigma} (^{(3)}R + K_{ab}K^{ab} - K^2)|N|\sqrt{q}\; d^3x\; dt \tag{12}$$

[6]. In doing this, we have neglected terms that result in boundary terms in (12). This can be justified by adding appropriate boundary counter-terms; these do not change the equations of motion or the physics. For detailed discussions of boundary terms, see [3, 6].

Next, we express (12) in terms of the phase space variables and their derivatives. For the rest of this sub-chapter, we follow [6]. The momenta are defined as functional derivatives of S with respect to the t derivatives of their conjugate variables. It can be shown that

$$\pi^{ab} = \frac{\delta S}{\delta \dot{q}_{ab}} = \frac{|N|}{2N}\sqrt{q}(K^{ab} - q^{ab}K). \tag{13}$$

Because the integrand of S is independent of $\dot{N}$ and $\dot{N^a}$, we have

$$\Pi = \frac{\delta S}{\delta \dot{N}} = 0, \qquad \Pi_a = \frac{\delta S}{\delta \dot{N^a}} = 0. \tag{14}$$

Hence, N and N^a are not dynamical [3]. The equations in (14) are re-written as

$$C(t,x) := \Pi(t,x) = 0, \qquad C^a(t,x) := \Pi^a(t,x) = 0 \quad \forall\, x \in \sigma. \tag{15}$$

In the language of P.A.M Dirac [26], these are called "primary constraints". Using these, (12) is re-cast as

$$S = \int_{-\infty}^{\infty} \int_{\sigma} \pi^{ab}\dot{q}_{ab} + \Pi\dot{N} + \Pi^a\dot{N}_a - (\lambda C + \lambda^a C_a + N^a H_a + |N|H) d^3x dt \tag{16}$$

where fields $\lambda(t,x)$ and $\lambda^a(t,x)$ are introduced and

$$H_a = -2q_{ac}D_b\pi^{bc},$$
$$H = \frac{2}{\sqrt{q}}(q_{ac}q_{bd} - \frac{1}{2}q_{ab}q_{cd})\pi^{ab}\pi^{cd} - \frac{\sqrt{q}R}{2}$$

are, respectively, the diffeomorphism and Hamiltonian constraints. Respectively, the diffeomorphism and Hamiltonian constraints correspond to (6) and (7) in the ADM formalism. λ and λ^a are also not dynamical; they are Lagrange multipliers that enforce the primary constraints upon requesting that their functional derivatives of S vanish. As in classical mechanics, we read off the Hamiltonian $\mathcal{H}$ straight from (16);

$$2\mathcal{H} := \int_{\sigma} \lambda C + \lambda^a C_a + N^a H_a + |N|H \; d^3x$$
$$= C[\lambda] + \tilde{C}[\underline{\lambda}] + \tilde{H}[\underline{N}] + H[|N|]$$

where C, $\tilde{C}$, $\tilde{H}$ and H are the functional, or smeared, versions of the constraints and $\underline{\lambda} := \lambda^a$ and $\underline{N} := N^a$. The functionals satisfy the following Poisson bracket relations:

$$\{\tilde{C}[\underline{f}], \mathcal{H}\} = \tilde{H}[\underline{f}], \quad \{C[f], \mathcal{H}\} = H\Big[\frac{N}{|N|} f\Big] \tag{17}$$

where f and $\underline{f}$ are some functions independent of t. However, the primary constraints must hold on-shell; this means that $\dot{C}[f] = \{\mathcal{H}, C[f]\} = 0 \; \forall f$ and similarly for $\tilde{C}[\underline{f}] \; \forall \underline{f}$. This gives

$$H(t,x) = 0, \quad H_a(t,x) = 0 \quad \forall \; x \in \sigma. \tag{18}$$

In the language of P.A.M Dirac [26], these are called "secondary constraints". The physical phase space $\mathcal{P}_{phys}$ is the subspace of $\mathcal{P}$ in which all constraints are satisfied [25]. In $\mathcal{P}_{phys}$, $\mathcal{H} = 0$. This is consistent with the lack of a global time in GR [25]. In [6], it is shown that $H[f]$ and $\tilde{H}[\underline{f}]$ satisfy the following Dirac algebra:

$$\begin{aligned}
\{\tilde{H}[\underline{f}], \tilde{H}[\underline{f}']\} &= -2\tilde{H}[\mathcal{L}_{\underline{f}} \underline{f'}], \\
\{\tilde{H}[\underline{f}], H[f]\} &= -2H[\mathcal{L}_{\underline{f}} f], \\
\{H[f], H[f']\} &= -2\tilde{H}[\underline{\underline{q}}^{-1}(f \underline{\partial f'} - f' \underline{\partial f})]
\end{aligned}$$

where the Poisson bracket is defined in [6] and $\mathcal{L}_{\underline{f}}$ is the Lie derivative on σ with respect to $\underline{f}$. In the language of P.A.M Dirac [26], these constraints are "first-class". This means that $\mathcal{P}_{phys}$ is closed under the transformations generated by the constraints [25]. Hence, this ensures that spacetime co-variance

in GR is preserved in the Hamiltonian formulation [25]. The functional Hamilton equations are equivalent to the vacuum Einstein field equations [25]. Hence, and as is fully discussed in [6], we have a Hamiltonian formulation of GR that corresponds to the Lagrangian formulation.

2.3 Ashtekar variables

The diffeomorphism and Hamiltonian constraints are highly non-linear in the phase space variables. This makes a direct quantisation of Hamiltonian GR difficult to accomplish. A breakthrough was made by Ashtekar [27, 28] who re-formulated Hamiltonian GR in terms of a set of variables that simplified the constraints. Nowadays, the variables are defined differently to those in [27, 28] (; see [29] for a review). For the rest of this sub-chapter, we follow the modern re-formulation of Hamiltonian GR in [6].

The metric q_{ab} on σ is written as

$$q_{ab} = \delta_{ij} e^i_a e^j_b \tag{19}$$

where e^i_a is the tetrad on σ and $i, \cdots \in \{1, 2, 3\}$ are $so(3)$ (or $su(2)$) indices. The inverse of e^i_a, denoted by e^a_i, is such that

$$e^i_a e^a_j = \delta^i_j, \qquad e^a_i e^i_b = \delta^a_b. \tag{20}$$

e^i_a is considered a one-form on σ into $su(2)$ because there is a local $SO(3)$ symmetry in (19); any pair of tetrads related by a $SO(3)$ transformation define the same metric q_{ab}. Part of this reasoning is that $so(3) \simeq su(2)$. The determinant of e^i_a, if it is viewed as a matrix with respect to its spatial and internal indices,

is given by $q = e^2$.

From the tetrad, the triad is defined as

$$E^a_i = \sqrt{q}\, e^a_i \tag{21}$$

and is a vector density on σ of weight 1 into $SU(2)$. The determinant of E^a_i, if it is viewed as a matrix, is given by $q = |E|$. Also, K_{ab} is expressed in terms of e^a_i and a one-form K^i_a on σ into $su(2)$ as

$$K_{ab} = K^i_{(a} e^i_{b)}. \tag{22}$$

It turns out [6] that the pair of phase space variables q_{ab} and π^{ab} may be replaced with the conjugate pair K^i_a and E^a_i. This extends $\mathcal{P}$ as the latter pair organically has more degrees of freedom than the former pair.

It is assumed that σ has a Levi-Civita connection D_a that is extended to act on simultaneous spatial and $so(3)$ tensors and be metric compatible with q_{ab} and e^i_a and, hence, E^a_i. The spin connection compatible with D_a is assumed to be Γ^i_a. From K^i_a and Γ^i_a, a $SU(2)$ connection is defined as

$$A^i_a := \Gamma^i_a + \gamma K^i_a. \tag{23}$$

The parameter γ is called the Immirzi parameter and generally is a complex number. Ashtekar's original choice was $\gamma = \pm i$ [27, 28], which gives the Ashtekar connection. However, Barbero [30] and Immirzi [31] allowed γ to be real. The value of γ does not fundamentally affect the classical theory but, as we will see in sub-chapters 4.2 and 6.1, the value of γ affects aspects of the quantum theory. It turns out [6] that A^i_a is compatible with a covariant derivative $\mathcal{D}_a$; we keep

the variance of these with γ implicit. $\mathcal{D}_a$ acts on simultaneous spatial and $so(3)$ tensors and is metric compatible with respect to ${}^{(\gamma)}E^a_i := \frac{E^a_i}{\gamma}$;

$$G_i := \mathcal{D}_a({}^{(\gamma)}E^a_i) = 0. \tag{24}$$

This imposes another constraint on $\mathcal{P}$ that is not present in the Hamiltonian formulation. It can be shown [6] that the constraint arises from the symmetry of K_{ab} and is first-class. We will further discuss this constraint shortly.

From the Poisson bracket relations between A^i_a and ${}^{(\gamma)}E^a_i$ [6], it can be seen that A^i_a and ${}^{(\gamma)}E^a_i$ are conjugate variables. A^i_a and its conjugate momentum ${}^{(\gamma)}E^a_i$ are the "Ashtekar variables" [29]. From K^i_a and E^a_i, a canonical transformation to the Ashtekar variables is performed. Hence, the Ashtekar variables replace K^i_a and E^a_i as variables on $\mathcal{P}$. It turns out [6] that the Ashtekar variables and ${}^{(\gamma)}K^i_a := \gamma K^i_a$ satisfy the following set of first-class constraints:

$$\begin{aligned}
G_i &= \mathcal{D}_a({}^{(\gamma)}E^a_i), \\
H_a &= F^i_{ab}\,{}^{(\gamma)}E^b_i, \\
H &= \left(\gamma^2 F^i_{ab} - (\gamma^2+1)\epsilon_{imn}\,{}^{(\gamma)}K^{m}_{a}\,{}^{(\gamma)}K^{n}_{b}\right)\frac{\epsilon_{ijk}\,{}^{(\gamma)}E^a_j\,{}^{(\gamma)}E^b_k}{\sqrt{|det({}^{(\gamma)}E\gamma)|}}
\end{aligned}$$

where F^i_{ab} is the curvature of A^i_a [6] and ϵ_{ijk} is the 3-index Levi-Civita symbol. The constraints are modulo terms in the new constraint, G_i, that do not change the definition of $\mathcal{P}_{phys}$ or that the constraints are first-class.

We now discuss the above constraints. The second and third expressions are, respectively, re-statements of the diffeomorphism and Hamiltonian constraints of Hamiltonian GR. The Hamiltonian constraint simplifies considerably

for Ashtekar's choice [27, 28] $\gamma = \pm i$ and this is the only case where the constraint is polynomial [32]. The remaining constraint, (24), resembles Gauss' law for electromagnetism and, hence, is called the Gauss constraint. The introduction of the Gauss constraint is a consequence of extending $\mathcal{P}$; the constraint keeps the number of physical degrees of freedom constant during the two changes of variables. Respectively, the Gauss and diffeomorphism constraints generate symmetries under $SU(2)$ gauge transformations and diffeomorphisms [2, 6]. The reader may notice that the $SO(3)$ symmetry from earlier has transmuted into a $SU(2)$ symmetry. To address this, we note that $SU(2)$ universally covers $SO(3)$. $SO(3)$ and $SU(2)$ correspond to the same symmetry classically but, to include spinors in the quantum theory, $SU(2)$ must be taken [33]. Although we will not couple the quantum theory to matter in this dissertation, we will allow for this by taking the $SU(2)$ symmetry. The Einstein-Hilbert action can be re-cast in terms of the Ashtekar variables [6].

The overall result is that, for $\gamma \in \mathbb{R}$, the re-formulation of Hamiltonian GR via the Ashtekar variables is a generalised Yang-Mills theory with $SU(2)$ gauge-invariance, diffeomorphism invariance and a vanishing on-shell Hamiltonian. This is the classical theory. Compared to the metric, ADM and Hamiltonian formulations, the construction of a quantum theory from the classical theory is much more feasible.

2.4 Reality conditions

In this sub-chapter, we follow [6]. The Ashtekar variables are real if γ is real and complex if γ is complex. For all values of γ, the Ashtekar variables must have the correct number of degrees of freedom. This happens if γ is real. For complex γ, including Ashtekar's choice [27, 28], the degrees of freedom of the Ashtekar variables are preserved by imposing the constraints below:

$$\frac{1}{\gamma}(A-\Gamma)-\overline{\frac{1}{\gamma}(A-\Gamma)}=0,$$
$$\frac{{}^{(\gamma)}E}{\gamma}-\overline{\left(\frac{{}^{(\gamma)}E}{\gamma}\right)}=0$$

where Γ is a non-analytic function of γ [6]. These are called reality conditions. Essentially, for $\gamma \in \mathbb{C}$, the complex Ashtekar variables are modified and the reality conditions demand that the modified variables have vanishing imaginary parts. The reality conditions preserve the $SU(2)$ gauge symmetry. The quantisation of the classical theory is most straightforward for $\gamma \in \mathbb{R}$ as the otherwise complicated reality conditions become trivial.

3 Quantisation

Now that we have set up the classical theory, we can discuss its quantisation. Background-independence of the quantum theory does not forbid the use of abstract manifolds in a quantisation procedure [34]. The classical theory must have a quantisation that is diffeomorphism-invariant [35]; this rules out a second-quantisation procedure. First, we review holonomies. Then, we briefly review past attempts at quantisation in the connection and loop representations. Our focus will be on the canonical quantisation of the classical theory which results in canonical LQG. From now on, apart from in sub-chapters 3.2 and 3.3, we take $\gamma \in \mathbb{R}$ to avoid the need to explicitly implement the reality conditions.

3.1 Holonomies

The introduction of holonomies will be needed for the quantum theory. We follow the presentation of [36]. In the rest of this dissertation, we let Σ be a differentiable and abstract 3D manifold. Further, let G be a gauge Lie group of finite dimension and g be its Lie algebra. To be consistent with our presentation in chapter 2, our review applies locally [36] and refers to an open neighbourhood of Σ. Let A be the connection on Σ into g,

$$A = A_a dx^a = A_a^I t^I dx^a, \tag{25}$$

where $\{x^a\}$ are local coordinates on Σ and $\{t^I\}_{I=1}^{dim(G)}$ are the generators of G. A path in the neighbourhood is a map $e : [s_1, s_2] \to \Sigma$, $s \to e(s)$, where $s \in [s_1, s_2] \subset \mathbb{R}$, that is continuous. We only consider paths that can be partitioned

into differentiable sections. A holonomy h_e into G is an object that is parallel transported along e,

$$\frac{d}{ds}h_e[A](s,s_1) = A_a(e(s))\frac{de^a}{ds}h_e[A](s,s_1), \qquad s_1 \leq s \leq s_2, \tag{26}$$

and satisfies $h_e(s_1,s_1) = I$ where I is the identity in G. (26) has a formal solution

$$h_e[A](s_2,s_1) = P\ exp\int_{s_1}^{s_2} A_a(e(t))\frac{de^a}{dt}dt \tag{27}$$

where P is the path ordering operator that acts on a product of n values of a function $f : [s_1,s_2] \to \mathbb{R}$ as

$$P(f(s_1)\dots f(s_n)) = f(s_{p_1})\dots f(s_{p_n}) \tag{28}$$

where $\{p_1,\dots,p_n\}$ is a permutation of $\{1,\dots,n\}$ such that $s_{p_1} \geq \dots \geq s_{p_n}$. Since A transforms as a connection under a gauge transformation $M(e)$ into G, h_e transforms homogeneously as

$$h_e(s_2,s_1) \to M(e(s_2))^{-1}h_e(s_2,s_1)M(e(s_1)) \tag{29}$$

where we have suppressed how h_e varies with A. A path l in Σ that has $s_1 = 0$, $s_2 = 1$ and $l(0) = l(1)$ is called a loop in Σ. A Wilson loop $W_l[A]$ of a loop l is the holonomy h_l traced over G;

$$W_l[A] := \frac{1}{\tilde{N}}\ Tr\ h_l[A] = \frac{1}{\tilde{N}}\ Tr\ Pexp\oint_l A \tag{30}$$

where $\tilde{N}$ is a normalisation factor. From (29), it can be seen that $W_l[A]$ is gauge invariant. It can be shown (,see [36] and references therein,) that the holonomies of a connection encode all physical information about the connection. This is an important property of the loop representation and the canonical quantisation.

3.2 The connection representation

The connection representation (CR) (, see [34] for a review,) is the analogue of the position representation in QM [37] with the Ashtekar connection A_a^i replacing the position. The triad E_i^a is treated as the conjugate momentum. The quantisation is performed by promoting A_a^i and E_i^a to operators, $\hat{A}_a^i$ and $\hat{E}_i^a$, that obey the Poisson bracket relations in [6] with $\{,\} \to \frac{1}{i}[,]$ [36]. The wave-functional $\psi[A]$ is expressed by $\langle A|$ of the connection bra space restricted to $\gamma = \pm i$ and $|\psi\rangle$ of the CR state ket space as

$$\psi[A] = \langle A|\psi\rangle \tag{31}$$

[38, 39]. The connection and triad operators act on $\psi[A]$ as

$$\hat{A}_a^i \psi[A] = A_a^i \psi[A],$$
$$\hat{E}_i^a \psi[A] = -i\frac{\delta}{\delta A_a^i}\psi[A]$$

[2] [34]. However, the CR encountered problems when $\gamma \neq \pm i$ because the Hamiltonian constraint is non-polynomial in this case [34]. Hence, we will not discuss the CR further.

3.3 The loop representation

The loop representation of quantum gravity (, see [40] for a review,) uses an over-complete [40] basis of Wilson loops to generate the space of "wave-functions" [40]. As Wilson loops are gauge invariant, they solve the quantised Gauss constraint. Wilson loops also solve the quantised Hamiltonian constraint [41]. For

Wilson loops to solve the quantised diffeomorphism constraint, they must divide into equivalence classes, under loop diffeomorphisms, given by knots [36]. A wave-function $\Psi(l)$ of a single loop l is expressed by $\langle l|$ of the loop bra space and $|\Psi\rangle$ of the loop representation state ket space as

$$\Psi(l) = \langle l|\Psi\rangle \tag{32}$$

[38]. The one-loop wave-functions determine wave-functions of multiple loops [40]. Analogous to the Fourier transform, the "loop transform" [39] expresses $\Psi(l)$ in terms of the wave-functionals $\psi[A]$ of the CR as

$$\Psi(l) = \int \overline{W_l[A]}\ \psi[A]\ d\mu(A) \tag{33}$$

where $\int d\mu(A)$ is the integral over the space of $SU(2)$ connections with measure $d\mu(A)$ (; see [39] and references therein). Because (33) includes complex $SU(2)$ connections, the reality conditions are non-trivial. Assuming that the diffeomorphism-equivalent Wilson loops [36] are used, $\Psi(l)$ satisfies the quantised Gauss and diffeomorphism constraints [40]. The quantised Hamiltonian constraint is more complicated and is treated in [40]. Despite the appealing properties of the loop representation, the inelegant over-completeness property and requirement for reality conditions are not ideal. Hence, we will not consider the loop representation further. Instead, we move on to the modern canonical approach of quantising the classical theory.

3.4 Constraints and Hilbert spaces in canonical quantisation

A central part of the canonical quantisation is to quantise and impose the Gauss, diffeomorphism and Hamiltonian constraints of the classical theory. Formally, we write the respective quantised constraints as

$$\hat{G}_i(x)\,|\Psi\rangle = 0,$$

$$\hat{H}_a(x)\,|\Psi\rangle = 0,$$

$$\hat{H}(x)\,|\Psi\rangle = 0 \qquad \forall\, x \in \Sigma.$$

We note that the quantised Hamiltonian constraint is a formal re-statement of the Wheeler-DeWitt equation [42]. Technically, each constraint consists of infinitely many constraints at all points in Σ but we will use these statements interchangeably. A physical state is $SU(2)$ gauge-invariant, diffeomorphism-invariant and is annihilated by the Hamiltonian constraint. Over the following five sub-sub-chapters, we will attempt to construct the physical Hilbert space by defining the "kinematical Hilbert space" [2] and implementing the constraints on it, one by one and top to bottom.

3.4.1 The kinematical Hilbert space

Let $\mathcal{G}$ be a graph, embedded in Σ, with n edges where each edge e has a holonomy $h_e[A]$ into $SU(2)$ and $\mathcal{G}$ is associated to a connection A. Also, let $\psi : SU(2)^n \to \mathbb{C}$ be a smooth function [43]. We define the "cylindrical function" [2] associated

with $\mathcal{G}$ and ψ as

$$\Psi_{\mathcal{G},\psi}[A] = \psi(h_{e_1}[A], \dots h_{e_n}[A]) \tag{34}$$

which is a functional of A into $\mathbb{C}$ [34, 37, 43]. The space of cylindrical functions with a common graph $\mathcal{G}$ is denoted by $Cyl_{\mathcal{G}}$ [43]. Also, the space of all cylindrical functions is $Cyl = \cup_{\mathcal{G}\in\Sigma}\, Cyl_{\mathcal{G}}$ [43]. À la QM, there is a correspondence between an abstract state $|\Psi_{\mathcal{G},\psi}\rangle$ and $\Psi_{\mathcal{G},\psi} \in Cyl$ via the unrestricted CR connection space;

$$\Psi_{\mathcal{G},\psi}[A] = \langle A|\Psi_{\mathcal{G},\psi}\rangle \tag{35}$$

[37]. The kinematical Hilbert space $\mathcal{K}$ [2] is defined as the complete space of states $|\Psi_{\mathcal{G},\psi}\rangle$, for all embedded graphs $\mathcal{G}$ in Σ and all functions ψ, equipped with the following scalar product [2];

$$\langle \Psi_{\mathcal{G},\psi}|\Psi_{\mathcal{G}',\chi}\rangle = \int_{SU(2)} \cdots \int_{SU(2)} \overline{\psi(U_1, \dots U_n)}\; \chi(U_1, \dots U_n)\; dU_n \dots dU_1 \tag{36}$$

where $\int_{SU(2)} dU$ is the integral over $SU(2)$ with Haar measure dU. The transformation law of the holonomy and the left and right invariance of the Haar measure mean that (36) is $SU(2)$ gauge-invariant [2]. (36) is also invariant under the group of "extended diffeomorphisms" $Diff^*(\Sigma)$ [2] [1] because these act only on cylindrical function graphs of which (36) is independent. That there are no negative-norm states in $\mathcal{K}$ is natural from the definition of (36) [34]. $\mathcal{K}$ is not separable as it has too many elements [2], including non-physical states that do not satisfy any constraint. However, this is not a problem as $\mathcal{K}$ is simply a step taken to get to the physical Hilbert space. To do this, the constraints are imposed on $\mathcal{K}$ by restricting to its Hilbert subspaces that satisfy them.

[1] $Diff^*(\Sigma)$ is chosen over $Diff(\Sigma)$ for reasons that will be explained later.

3.4.2 Imposing the Gauss constraint

We define the Hilbert subspace of $\mathcal{K}$ that solves the Gauss constraint as the $SU(2)$ gauge-invariant space $\mathcal{K}_{SU(2)}$ [43]. $\mathcal{K}_{SU(2)}$ inherits the scalar product in (36). It can be shown [43, 39] that $\mathcal{K}_{SU(2)}$ has a complete, linearly independent and orthonormal basis consisting of spin network states. A spin network is a generalisation of the Wilson loop that has a graph $\mathcal{G}$ with vertices and edges that encode the $SU(2)$ group. Spin networks naturally resolve the over-completeness of Wilson loops. To understand $\mathcal{K}_{SU(2)}$, it is sufficient to understand the spin network basis states. We will further discuss spin networks in sub-chapter 4.1.

3.4.3 Imposing the diffeomorphism constraint

We define $\mathcal{K}_{diff}$ as the Hilbert subspace of $\mathcal{K}$ invariant under gauge $SU(2)$ and $Diff^*(\Sigma)$ [2]. Spin network states, apart from the trivial state [34], are mapped to different spin network states under $Diff^*(\Sigma)$ [2]. Hence, non-trivial states in $\mathcal{K}_{SU(2)}$ are not diffeomorphism-invariant. We want to find the non-trivial states in $\mathcal{K}_{diff}$.

Firstly, we note that $Cyl \subset \mathcal{K} \subset Cyl^*$ [43] where Cyl^* is the space of "distributional states" [34, 43] dual to Cyl. However, if we wanted to proceed by analogy with our discussion of $\mathcal{K}$, we would encounter difficulties. We can neither explicitly define a scalar product in the same way nor can we construct states that manifest $Diff^*(\Sigma)$ invariance [34, 2]. Both of these need a measure on $Diff^*(\Sigma)$ for which there is no explicit construction [34]. Instead, we implement the idea of "summing over $Diff^*(\Sigma)$" in a different way. For the rest of the

construction of $\mathcal{K}_{diff}$, we follow [43]. Elements of $Diff^*(\Sigma)$ act on $\Psi_{\mathcal{G},\psi} \in Cyl$ as

$$U(\phi)\Psi_{\mathcal{G},\psi} = U(\phi)\Psi_{\phi^{-1}\mathcal{G},\psi} \tag{37}$$

where $U(\phi)$ is the unitary operator corresponding to $\phi \in Diff^*(\Sigma)$. The action of $Diff^*(\Sigma)$ on Cyl^* is defined through that on Cyl [2]. Hence, the diffeomorphism constraint is imposed on Cyl^* as

$$(\Psi|U(\phi) = (\Psi| \quad \forall\ \phi \in Diff^*(\Sigma). \tag{38}$$

Elements of Cyl^* that satisfy (38) are in $\mathcal{K}_{diff}$.

We consider the following distributional state;

$$(\Psi_{\mathcal{G},\psi}| = \sum_{\phi \in Diff^*(\Sigma)} \langle \Psi_{\mathcal{G},\psi}|\, U(\phi) \tag{39}$$

where the elements $\{\langle \Psi_{\mathcal{G},\psi}|\}$ belong to the bra space corresponding to Cyl. The scalar product of $(\Psi_{\mathcal{G},\psi}|$ and an element $|\Psi_{\mathcal{G}',\chi}\rangle$ of the ket space of Cyl is a finite sum [43, 2]. Hence, $(\Psi_{\mathcal{G},\psi}|$ is a well-defined element of Cyl^*. Since $(\Psi_{\mathcal{G},\psi}|$ solves (38), it is an element of $\mathcal{K}_{diff}$. Hence, we have a construction for the set of elements in $\mathcal{K}_{diff}$. The scalar product on $\mathcal{K}_{diff}$ is induced by that on $\mathcal{K}_{SU(2)}$ as

$$\langle \Psi_{\mathcal{G},\psi}|\Psi_{\mathcal{G}',\chi}\rangle_{diff} = (\Psi_{\mathcal{G},\psi}\,|\Psi_{\mathcal{G}',\chi}\rangle \tag{40}$$

and is invariant under $Diff^*(\Sigma)$. Hence, $\mathcal{K}_{diff}$ is defined by "summing over $Diff^*(\Sigma)$".

$\mathcal{K}_{diff}$ has a complete [39], discrete and orthonormal [2] basis consisting of s-knot states [2]. A s-knot state $|s\rangle$ is a set of spin network states whose spin

network graphs are equivalent under $Diff^*(\Sigma)$. To this end, s-knot states are labelled by $Diff^*(\Sigma)$-equivalent knots [2]. Because the s-knot basis is discrete, $\mathcal{K}_{diff}$ is separable [2]. [2] As we will discuss later, s-knots are quantum states of space.

The construction of $\mathcal{K}_{diff}$ and the loop representation have indicated a remarkable link between quantum gravity and knot theory. For more on this relation, see [44].

3.4.4 Imposing the Hamiltonian constraint

In the canonical formulation of LQG, the Hamiltonian governs both the dynamics and the physical Hilbert space. The physical Hilbert space $\mathcal{H}$ is the subspace of $\mathcal{K}_{diff}$ that satisfies the Hamiltonian constraint and has an appropriate scalar product. The Hamiltonian constraint is the hardest one to implement. This is because the classical Hamiltonian is difficult to quantise due to its non-linearity in the Ashtekar variables. Also, because the Dirac algebra is not a proper Lie algebra, the action of $\hat{H}$ on $\mathcal{K}_{diff}$ is not closed [6].

A construction of the Hamiltonian operator is presented by Thiemann in [45, 46]. Thiemann also proposes a physical Hilbert space in [45, 47]. The resulting Hamiltonian is totally well-defined and the corresponding Hamiltonian constraint can admit exact solutions [45, 46, 47]. Thiemann's construction is significant and appealing as it directly pertains to LQG. However, the resulting operator has the closure problem [48]. Also, there are ambiguities in how the

[2] If $Diff(\Sigma)$ was used instead of $Diff^*(\Sigma)$, the opposite would be true [2].

Hamiltonian operator is defined [45, 46, 47, 2] in that there are two different forms and no unique regularisation. Furthermore, Thiemann's construction has been challenged for not semi-classically reducing to GR [49], resulting in states that do not satisfy the diffeomorphism constraint [50] and inconsistencies in the resulting constraint algebras [51]. The form of the Dirac algebra is responsible for the issues of inconsistency and closure [48]. Other ways of constructing the Hamiltonian operator can be found in the references in this sub-sub-chapter and references therein.

3.4.5 The master constraint

Thiemann [48] attempted to address problems highlighted in the previous sub-sub-chapter by introducing the classical object

$$\mathbf{M} = \int_{\Sigma} \frac{H(x)^2}{\sqrt{q(x)}}\, d^3x. \tag{41}$$

This is called the master constraint [48]. It is equivalent to the set of all Hamiltonian constraints [48, 6];

$$\mathbf{M} = 0 \quad \leftrightarrow \quad H(x) = 0 \ \ \forall\, x \in \Sigma. \tag{42}$$

$\mathbf{M}$ and $\tilde{H}(\underline{N})$ satisfy the following Poisson bracket algebra on Σ [6]:

$$\{\tilde{H}[\underline{N}], \tilde{H}[\underline{N}']\} = -2\tilde{H}[\mathcal{L}_{\underline{N}}\underline{N}'],$$

$$\{\tilde{H}[\underline{N}], \mathbf{M}\} = 0,$$

$$\{\mathbf{M}, \mathbf{M}\} = 0.$$

Compared to the Dirac algebra, the above is much simpler and is a Lie algebra [48]. Furthermore, because $H(x)$ and $q(x)$ are, respectively, scalar densities of weight 1 and 2, the integrand of $\mathbf{M}$ is a scalar density of weight 1. Hence, $\mathbf{M}$ is invariant under spatial diffeomorphisms [48]. Thus, unlike ordinary Hamiltonian constraints including those in [45, 46, 47], the quantised master constraint [48] can be imposed directly onto $\mathcal{K}_{diff}$ and is closed on $\mathcal{K}_{diff}$. This means that the master constraint [48] is free from the problems and ambiguities encountered in [45, 46, 47].

The properties of the master constraint [48] make it easier and more elegant to quantise than ordinary Hamiltonian constraints. Upon quantisation, the object considered is actually a positive and closed quadratic form $Q_{\mathbf{M}}$ [48]. It is shown [52] that $Q_{\mathbf{M}}$ is uniquely determined by a master constraint operator $\hat{\mathbf{M}}$ that is positive and self-adjoint. Given this, the separability of $\mathcal{K}_{diff}$ implies [48, 6] that it decomposes as

$$\mathcal{K}_{diff} = \int_{\mathbb{R}}^{\oplus} \mathcal{K}^{\oplus}_{diff}(\lambda)\, d\mu(\lambda) \tag{43}$$

where $\mathcal{K}^{\oplus}_{diff}(\lambda)$ is a Hilbert eigenspace of $\hat{\mathbf{M}}$ with real eigenvalue λ and scalar product induced by $\mathcal{K}_{diff}$ and $d\mu(\lambda)$ is an appropriate measure. This means that $\mathcal{H} = \mathcal{K}^{\oplus}_{diff}(0)$ [48] as $\mathcal{K}^{\oplus}_{diff}(0)$ has eigenvalue 0. Hence, the master constraint programme [48] serves as a proposal for the Hamiltonian constraint and physical Hilbert space. The master constraint works for various systems other than LQG that have finitely and infinitely many degrees of freedom (; see [53] and the four prequels referenced therein). This provides evidence that the master constraint method [48] is valid. However, this has not been formally proved.

We note, through the discussions in this chapter and [34], that the definitions of the Hamiltonian constraint and physical Hilbert space are ambiguous. In the next chapter, we will discuss certain operators in canonical LQG.

4 Aspects of canonical loop quantum gravity

In this chapter, we review properties of the spin network basis of LQG. We will also review the LQG area and volume operators and their eigenspectra. In addition, we will review the quantisation of space in LQG.

4.1 Properties of spin networks

This sub-chapter follows from sub-sub-chapter 3.4.2. Firstly, we give a definition of a spin network [54] for a general gauge Lie group G. A spin network is a graph $\mathcal{G}$ where each edge e is assigned a holonomy h_e and each node v is assigned an intertwiner I_v. The holonomies are generalised from those in sub-chapter 3.1 as each one transforms in some irreducible representation (irrep) of G. The intertwiners are G-invariant tensors. Since LQG uses $SU(2)$ spin networks, we will assume them in this chapter but general spin networks will arise in chapter 5.

The irreps of $SU(2)$ are labelled by $j \in \frac{1}{2}\mathbb{N}$ and we will call these spin-j irreps. We denote a generalised holonomy of a spin network edge e transforming in the spin-j_e irrep ρ_{j_e} as $\rho_{j_e}(h_e)$ [34]. This is a matrix with elements labelled by $m, \cdots \in \{-j_e, -(j_e-1), \ldots, j_e-1, j_e\}$.

Let an intertwiner I_v of a node v have a outgoing edges and b incoming edges. I_v can be viewed [54] as a type (a, b) $SU(2)$-invariant tensor that has a upper m-type indices and b lower m-type indices. The valence of v is $a+b$. An n-valent intertwiner is an intertwiner of a node of valence n. The 3-valent intertwiner can be chosen as the $SU(2)$ Wigner $3j$ symbol [54]. The n-valent intertwiner

can be expressed in terms of 3-valent intertwiners [54]. G intertwiners also have tensorial structures.

A spin network with N edges has the cylindrical function

$$\Psi_{\{\mathcal{G},\{j_e\},\{i_v\}\}}[h_{e_1},\ldots,h_{e_N}] = \Big(\prod_{v\in\mathcal{G}} I_v\Big)\Big(\prod_{e\in\mathcal{G}} \rho_{j_e}(h_e)\Big) \tag{44}$$

where all m-type indices are implicit and contracted as in [54].

Spin networks have a physical and an abstract interpretation [33]. Physically, they are embedded in Σ and correspond to possible states of space as we will discuss in sub-chapter 4.4. Abstractly, they encode quantities and representations of $SU(2)$ in a background-independent way.

If all nodes of an abstract spin network are tri-valent, it is subject to the properties in [55, 56] that constrain the spins of the edges [33].

Spin networks are very practical for performing calculations. The graphical calculus of Kauffman-Lins re-coupling theory [57] is nicely tailored to them. In the re-coupling theory, it is customary to label the edges of spin networks by numbers of the form $p = 2j$. Moreover, the spin network basis diagonalises the area and volume operators. Over the next two sub-chapters, we will demonstrate how practical the spin network basis is in analysing the area and volume operators.

4.2 The area operator

We now discuss the area operator in LQG. Let $\mathcal{S}$ be a 2D surface embedded in Σ via $\sigma^u \to x^a(\sigma)$ where $\sigma^u = (\sigma^1, \sigma^2)$ are coordinates on $\mathcal{S}$. The area of $\mathcal{S}$ is

[58]

$$\mathcal{A}(\mathcal{S}) = \int\int_{\mathcal{S}} \sqrt{\phi * q}\; d^2\sigma \tag{45}$$

where $\phi * q$ is the determinant of the pull-back of q_{ab} to $\mathcal{S}$. $\mathcal{A}(\mathcal{S})$ is $SU(2)$ gauge-invariant, due to the invariance of the integrand, but is not diffeomorphism-invariant [2]. Hence, the operator corresponding to $\mathcal{A}(\mathcal{S})$ is defined on $\mathcal{K}_{SU(2)}$ [2]. We can write $\mathcal{A}(\mathcal{S})$ in terms of the Ashtekar variables as [58]

$$\mathcal{A}(\mathcal{S}) = \int\int_{\mathcal{S}} \sqrt{n_a n_b E^a_i E^b_i}\; d^2\sigma. \tag{46}$$

If $\mathcal{A}(\mathcal{S})$ were promoted to an operator à la the CR, the result would be ill-defined. Instead, we must carry out a background-independent regularisation procedure for $\mathcal{A}(\mathcal{S})$. For the rest of this sub-chapter, we follow [2]. In doing so, we will keep γ implicit and re-introduce it near the end of this sub-chapter.

The regularisation procedure of [2] starts by appending a third dimension to $\mathcal{S}$ by definition of a third coordinate $\xi \in [-\frac{\delta}{2}, \frac{\delta}{2}]$ with infinitesimal δ. This defines a 3D region $\tilde{\mathcal{S}}$, coordinatised by $x^a = (\sigma^u, \xi)$, whose $\xi = 0$ hypersurface is $\mathcal{S}$. Next, $\tilde{\mathcal{S}}$ is split into cuboids $\{B_{I\epsilon}\}$, labelled by the index I, with infinitesimal side length $\epsilon > 0$ and height δ where $\delta = \epsilon^k$ and $1 < k < 2$. The choice of k will be explained later. The area $\mathcal{A}_{I\epsilon}(\xi)$ of the square intersection between $B_{I\epsilon}$ and a constant ξ hypersurface is defined as

$$\mathcal{A}_{I\epsilon}(\xi) = \int\int_{B_{I\epsilon} \cap \{\xi \,=\, constant\}} \sqrt{n_a n_b E^a_i E^b_i}\; d^2\sigma. \tag{47}$$

The average of $\{\mathcal{A}_{I\epsilon}(\xi)\}$ over $B_{I\epsilon}$ is defined as

$$\mathcal{A}_{I\epsilon} = \frac{1}{\delta}\int_{-\frac{\delta}{2}}^{\frac{\delta}{2}} \mathcal{A}_{I\epsilon}(\xi)\; d\xi = \frac{1}{\delta}\int_{B_{I\epsilon}} \sqrt{n_a n_b E^a_i E^b_i}\; d^3x. \tag{48}$$

It is the case that

$$\mathcal{A}_{I\epsilon} = \sqrt{\mathcal{A}_{I\epsilon}^2} \tag{49}$$

where, as $\mathcal{A}_{I\epsilon} > 0$, the positive root is taken. It can be shown [2] that

$$\mathcal{A}_{I\epsilon}^2 = \frac{1}{2\delta^2} \int_{B_{I\epsilon}} \int_{B_{I\epsilon}} n_a(x) n_b(y) T^{ab}(x,y)\, d^3y\, d^3x + \mathcal{O}(\epsilon^5) \tag{50}$$

where n^a is the vector field normal to $\tilde{\mathcal{S}}$ and the "two handed loop quantity" T^{ab} is

$$T^{ab}(x,y) = E_i^a(x) \rho_1(h_l)^{ij} E_j^b(y) \tag{51}$$

where ρ_1 is the adjoint representation of $SU(2)$ and x and y are joined by the line l. x and y are the "hands" [2] of T^{ab}. The average area $\mathcal{A}_\epsilon(\mathcal{S})$ of the constant ξ hypersurfaces in $\tilde{\mathcal{S}}$ is defined as

$$\mathcal{A}_\epsilon(\mathcal{S}) = \sum_I \mathcal{A}_{I\epsilon}. \tag{52}$$

This is a Riemann sum over cuboids that covers the interior of $\tilde{\mathcal{S}}$ [58]. To only cover $\mathcal{S}$, we must get rid of the third dimension by letting $\epsilon \to 0$. In this limit, the Riemann sum approaches [58]

$$\mathcal{A}(\mathcal{S}) = \lim_{\epsilon \to 0} \mathcal{A}_\epsilon(\mathcal{S}). \tag{53}$$

$\mathcal{A}(\mathcal{S})$ is now regularised thanks to the background-independent regularisation. $\mathcal{A}(\mathcal{S})$ and its associated quantities, (49) - (53), can now be promoted to opera-

tors;

$$\hat{\mathcal{A}}(\mathcal{S}) = \lim_{\epsilon \to 0} \hat{\mathcal{A}}_\epsilon(\mathcal{S}),$$
$$\hat{\mathcal{A}}_\epsilon(\mathcal{S}) = \sum_I \hat{\mathcal{A}}_{I\epsilon},$$
$$\hat{\mathcal{A}}_{I\epsilon} = \sqrt{\hat{\mathcal{A}}^2_{I\epsilon}},$$
$$\hat{\mathcal{A}}^2_{I\epsilon} = \frac{1}{2\delta^2} \int_{B_I} \int_{B_I} n_a(x) n_b(y) \hat{T}^{ab}(x,y)\, d^3y\, d^3x.$$

The area operator $\hat{\mathcal{A}}(\mathcal{S})$ is well-defined. In the fourth expression, $\mathcal{O}(\epsilon^5)$ terms are neglected because they vanish as $\epsilon \to 0$.

The action of $\hat{\mathcal{A}}(\mathcal{S})$ on a spin network state, denoted by $|S\rangle$, is then sought. $\hat{\mathcal{A}}(\mathcal{S})$ does not change the spin network graph $\mathcal{G}$. The action of the "two-handed loop operator" [2] $\hat{T}^{ab}(x,y)$ on $|S\rangle$ is only non-zero if x and y are both on edges of $\mathcal{G}$. We say that the hands "hold" $\mathcal{G}$. Also, in $\hat{\mathcal{A}}(\mathcal{S})$, the hands of $\hat{T}^{ab}$ cover all of $\mathcal{S}$. Hence, the action of $\hat{\mathcal{A}}(\mathcal{S})$ on $|S\rangle$ is only non-zero where the hands of $\hat{T}^{ab}$ hold $\mathcal{G}$ and $\mathcal{S}$ simultaneously. Hence, $\hat{\mathcal{A}}(\mathcal{S})\,|S\rangle$ only depends on the intersections of $\mathcal{S}$ with $\mathcal{G}$.

An intersection ι, which is technically 2-valent, can be considered n-valent without losing generality. ι will have edges above, below and tangential to $\mathcal{S}$. Respectively, we call these A,B and T edges. As $\epsilon \to 0$, ι will be in one of the cuboids $B_{I\epsilon}$. In the corresponding operator $\hat{\mathcal{A}}^2_{I\epsilon}$, the hands of $\hat{T}^{ab}$ cover all of $B_{I\epsilon}$. $\hat{T}^{ab}$ acts non-trivially on $|S\rangle$ by holding an edge in each hand, or holding one edge with both hands, and forming a joining edge labelled by $p = 2$ (up to an overall factor). Because $\hat{T}^{ab}$ holds 2 edges from a choice of n, the action of

$\hat{T}^{ab}$ on $|S\rangle$ is a sum of n^2 terms. However, in the limit that $\epsilon \to 0$, some of these vanish [2]. Hence, the action of $\hat{\mathcal{A}}^2_{I\epsilon}$ on $|S\rangle$ is a sum of terms and, as it turns out [2], each non-zero term has the limiting value

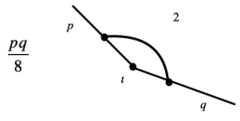

. This is proportional to a recoupling diagram whose joined edges have labels p and q and the other edges are untouched. As $k > 1$, the angles between $\mathcal{S}$ and the edges are irrelevant.

"Macroscopically", ι appears to be a n-valent node. "Microscopically", ι can be viewed as having a trivalent structure with virtual trivalent nodes joined by virtual A, B and T edges. Ultimately, the virtual edges join to the real A, B and T edges of ι seen from the "macroscopic" view. This "microscopic" structure can be viewed as a consequence of the trivalent structure of the n-valent intertwiner. "Microscopically", ι is trivalent and joined to other virtual nodes by a virtual A edge, a virtual B edge and a virtual T edge. The "microscopic" structure of ι is

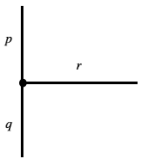

where the other virtual trivalent nodes are not shown and, respectively, the virtual A,B and T edges joined to ι are labelled by p, q and r. From here, we identify the edges in the diagram by their labels. The p, q and r edges are

special; it can be shown [2] that the holds that $\hat{T}^{ab}$ has on any other A and B edges can be moved to the p and q edges. Further, it turns out [2] that, as $k < 2$, no T edges contribute as $\epsilon \to 0$. As $\epsilon \to 0$, the action of $\hat{\mathcal{A}}^2_{I_\epsilon}$ approaches that of the squared area operator at ι, $\hat{\mathcal{A}}^2_\iota$.

With consideration of all of these ideas, as $\epsilon \to 0$, the action of $\hat{\mathcal{A}}^2_\iota$ on ι is

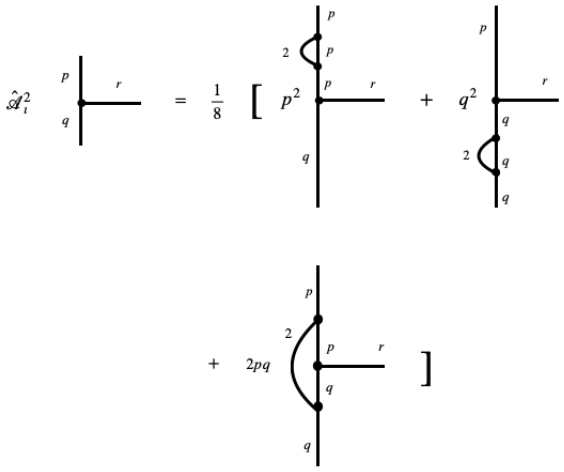

. There are three possible terms. Each consist of a combination of ι and the recoupling diagram from earlier. The first has the p edge self-joined. The second has the q edge self-joined and is the first with p and q switched. The third has the p and q edges joined and is symmetric in p and q so gets a factor of 2. Each term is a multiple of ι. The constants of proportionality for each of the first and second terms can be found by isolating the θ net joined to two open edges and using the reduction formulae [58]. The other constant must be found by closing the diagrams in the proportionality relation and solving the resulting equation. Closing ι gives θ and closing the third term gives Tet [58].

The constants of proportionality are given in [2]. Hence, ι is an eigenfunction of $\hat{\mathcal{A}}_\iota^2$ with eigenvalue

$$\frac{\gamma^2}{4}\Big(2(\frac{p}{2})(\frac{p}{2}+1)+2(\frac{q}{2})(\frac{q}{2}+1)-\frac{r}{2}(\frac{r}{2}+1)\Big)$$
$$=\frac{\gamma^2}{4}\Big(2j_\iota^u(j_\iota^u+1)+2j_\iota^d(j_\iota^d+1)-j_\iota^t(j_\iota^t+1)\Big)$$

where $j_\iota^u=\frac{p}{2}$, $j_\iota^d=\frac{q}{2}$ and $j_\iota^t=\frac{r}{2}$ and γ has been re-instated. Hence, the spin network basis diagonalises $\hat{\mathcal{A}}_\iota^2$ and, hence, $\hat{\mathcal{A}}_\iota$. Thus, ι is an eigenfunction of $\hat{\mathcal{A}}_\iota$ with eigenvalue

$$\sqrt{\frac{\gamma^2}{4}\Big(2j_\iota^u(j_\iota^u+1)+2j_\iota^d(j_\iota^d+1)-j_\iota^t(j_\iota^t+1)\Big)}$$
$$=\frac{\gamma}{2}\sqrt{2j_\iota^u(j_\iota^u+1)+2j_\iota^d(j_\iota^d+1)-j_\iota^t(j_\iota^t+1)}. \tag{54}$$

To get $\hat{\mathcal{A}}(\mathcal{S})\,|S\rangle$, the action of $\hat{\mathcal{A}}_\iota$ on ι is summed over all ι;

$$\hat{\mathcal{A}}(\mathcal{S})\,|S\rangle=\Big(\frac{\gamma}{2}\sum_{\iota\in\mathcal{G}\cap\mathcal{S}}\sqrt{2j_\iota^u(j_\iota^u+1)+2j_\iota^d(j_\iota^d+1)-j_\iota^t(j_\iota^t+1)}\Big)\,|S\rangle\,. \tag{55}$$

If $j_\iota^u=j_\iota^d=j_\iota$ and $j_\iota^t=0$, there is a special case;

$$\hat{\mathcal{A}}(\mathcal{S})\,|S\rangle=\Big(\gamma\sum_{\iota\in\mathcal{G}\cap\mathcal{S}}\sqrt{j_\iota(j_\iota+1)}\Big)\,|S\rangle\,. \tag{56}$$

The eigenspectrum of $\hat{\mathcal{A}}(\mathcal{S})$ is quantised. It is labelled by $j_i=(j_i^u,j_i^d,j_i^t)$ where $i\in\{1,\dots n\}$. The area eigenvalues of (55) but not of (56) are degenerate. The spectrum of $\hat{\mathcal{A}}(\mathcal{S})$ should be observable. There is a minimum area eigenvalue in the non-degenerate sector with $j_\iota=\frac{1}{2}$; $\Delta=\frac{\sqrt{3}}{2}\gamma$. This is the area gap and is the smallest possible area in LQG. These predictions are consistent with quantum gravity. The classical theory has the limit that $\Delta\to 0$. The fact that γ determines the observable Δ shows that the value of γ matters in the quantum theory.

4.3 The volume operator

We now discuss the volume operator in LQG. Due to the increased complexity of the calculations from the area operator, the mathematical analysis of the volume operator will be more schematic. For the rest of this sub-chapter, we follow [58]. We will see that the area and volume operators share several properties.

The volume of a 3D region $\mathcal{R} \in \Sigma$ is

$$V(\mathcal{R}) = \int \int \int_{\mathcal{R}} \sqrt{\phi * q}\, d^3x \tag{57}$$

where $\phi * q$ is the determinant of the pull-back of q_{ab} to $\mathcal{R}$. Like the area operator, the volume operator of $\mathcal{R}$ is a $\mathcal{K}_{SU(2)}$ operator. In terms of the Ashtekar variables,

$$V(\mathcal{R}) = \int \int \int_{\mathcal{R}} \sqrt{\frac{1}{3!}|\epsilon_{abc}\epsilon_{ijk}E^{ai}E^{bj}E^{ck}|}\, d^3x. \tag{58}$$

Again, we must regularise $V(\mathcal{R})$ background-independently. The regularisation in [58] starts with the "three-handed loop variable" [58] $T^{abc}(x, r, s, t)$ [2], a generalisation of the two-handed quantity with three hands r, s and t, each joined by a straight line to x. Next, $\mathcal{R}$ is discretised into a 3D grid of cubes $\{C_{I\epsilon}\}$, labelled by I, of side length $\epsilon > 0$. [58] defines the following object associated to $C_{I\epsilon}$;

$$W_{I\epsilon}(x) = \frac{1}{16\ 3!\epsilon^6} \int_{\partial C_{I\epsilon}} \int_{\partial C_{I\epsilon}} \int_{\partial C_{I\epsilon}} |n_a(\rho)n_b(\sigma)n_c(\tau)T^{abc}(x, \rho, \sigma, \tau)|\ d^2\tau\ d^2\sigma\ d^2\rho \tag{59}$$

[2] where n^a is the normal vector field to $C_{I\epsilon}$ and ρ^u, σ^u and τ^u are sets of coordinates on $\partial C_{I\epsilon}$. It can be shown [58, 2] that, as $\epsilon \to 0$, $W_{I\epsilon}$ approaches

$E(x_I) = q(x_I)$ for fixed $x_I \in C_{I\epsilon}$. Hence, as $\epsilon \to 0$, $\sqrt{W_{I\epsilon}} \to \sqrt{q(x_I)}$, the factor that scales the volume of $C_{I\epsilon}$ as for ordinary Riemannian manifolds. Thus, in the limit that $\epsilon \to 0$, $\epsilon^3\sqrt{W_{I\epsilon}}$ is the volume of $C_{I\epsilon}$. The volume of $\mathcal{R}$ is estimated by the Riemann sum of the volumes of $\{C_{I\epsilon}\}$;

$$V_\epsilon(\mathcal{R}) = \sum_I \epsilon^3 \sqrt{W_{I\epsilon}}. \tag{60}$$

As before, the Riemann sum converges in the limit to

$$V(\mathcal{R}) = \lim_{\epsilon \to 0} V_\epsilon(\mathcal{R}). \tag{61}$$

This successfully regularises $V(\mathcal{R})$. $V(\mathcal{R})$ and its defining quantities, (59) - (61), are then promoted to operators [2];

$$\begin{aligned}
&\hat{V}(\mathcal{R}) = \lim_{\epsilon \to 0} \hat{V}_\epsilon(\mathcal{R}), \\
&\hat{V}_\epsilon(\mathcal{R}) = \sum_I \epsilon^3 \sqrt{\hat{W}_{I\epsilon}}, \\
&\hat{W}_{I\epsilon} = \frac{1}{16\ 3!\epsilon^6} \int_{\partial C_{I\epsilon}} \int_{\partial C_{I\epsilon}} \int_{\partial C_{I\epsilon}} |n_a(\rho) n_b(\sigma) n_c(\tau) \hat{T}^{abc}(x, \rho, \sigma, \tau)|\ d^2\tau\ d^2\sigma\ d^2\rho.
\end{aligned}$$

The volume operator $\hat{V}(\mathcal{R})$ is well-defined and the factors of ϵ^6 cancel.

The action of $\hat{V}(\mathcal{R})$ on spin network states is then examined. Like the area operator, $\hat{V}(\mathcal{R})$ does not change the graph $\mathcal{G}$ of $|S\rangle$. Also, $\hat{V}(\mathcal{R})$ does not change the spins or holonomies of S. Hence, the action of $\hat{V}(\mathcal{R})$ is only non-trivial on the nodes [2]. The hands and lines of the "three handed loop operator" [2] $\hat{T}^{abc}(x, r, s, t)$ can, respectively, be considered nodes and edges of a graph corresponding to $\hat{T}^{abc}$. $\hat{T}^{abc}$ annihilates $|S\rangle$ unless the three hands of $\hat{T}^{abc}$ hold $\mathcal{G}$. In $\hat{W}_{I\epsilon}$, the hands of $\hat{T}^{abc}$ are independent and individually cover

$\partial C_{I\epsilon}$. Hence, $\hat{W}_{I\epsilon}$ annihilates $|S\rangle$ unless each hand holds an intersection of $\mathcal{G}$ with $\partial C_{I\epsilon}$; this happens at three points where the lines of the graph of $\hat{T}^{abc}$ intersect $\partial C_{I\epsilon}$. Since each hand individually covers $\partial C_{I\epsilon}$, it can hold any of the three intersections. Hence, $\hat{W}_{I\epsilon}|S\rangle$ reduces to a sum of 3^3 terms. However, symmetry restrictions [58] mean that a term vanishes unless all three hands of $\hat{T}^{abc}$ hold different intersections. Furthermore, there is a cancellation between terms with only two intersections [58]. Hence, $\hat{W}_{I\epsilon}|S\rangle$ becomes a sum over triplets of different intersections. For a cube C^v_ϵ enclosing a node v of $\mathcal{G}$, this is

$$\langle S|\,\hat{W}_{C^v_\epsilon} = \frac{i(\sqrt{2})^6}{16\ 3!\epsilon^6} \sum_{\{r,s,t\}} \langle S_{\{r,s,t\}}| \tag{62}$$

where $\{r,s,t\}$ is a triplet of different points in $\mathcal{G}\cap\partial C^v_\epsilon$ and $\langle S_{rst}|$ is $\langle S|$ held by the hands r, s and t of $\hat{T}^{abc}$. $\langle S|\,\hat{V}_\epsilon(\mathcal{R})$ becomes a sum over cubes with at least three different surfacial intersections; these are exclusively C^v_ϵ as $\epsilon\to 0$. Hence, $\langle S|\,\hat{V}_\epsilon(\mathcal{R})$ becomes a sum over nodes of $\mathcal{G}$ in $\mathcal{R}$;

$$\langle S|\,\hat{V}_\epsilon(\mathcal{R}) = \sum_{v\in\mathcal{G}\cap\mathcal{R}} \epsilon^3\,\langle S|\,\sqrt{|\hat{W}_{C^v_\epsilon}|}. \tag{63}$$

Thus, it is the case that

$$\langle S|\,\hat{V}(\mathcal{R}) = \lim_{\epsilon\to 0} \sum_{v\in\mathcal{G}\cap\mathcal{R}} \epsilon^3\,\langle S|\,\sqrt{|\hat{W}_{C^v_\epsilon}|}. \tag{64}$$

It can be shown [58] that

$$\hat{V}(\mathcal{R})\,|S\rangle = (\sqrt{2})^3 \sum_{v\in\mathcal{G}\cap\mathcal{R}} \sqrt{\sum_{r,t,s} |\frac{i}{16}\hat{W}^{n_v}_{[rts]}|}\,|S\rangle \tag{65}$$

where the sum in the square root is over $r\in\{0,\ldots,n_v-3\}$, $t\in\{r+1,\ldots,n_v-2\}$ and $s\in\{t+1,\ldots,n_v-1\}$, n_v is the valence of v and $\{\hat{W}^{n_v}_{[rts]}\}$ are three-handed

operators holding edges joined to v. By recoupling theory, $\hat{W}_{C_\epsilon^v}$ is related to $\{\hat{W}^{n_v}_{[rts]}\}$ which are related to a set of matrices $\{W^{n_v}_{[rts]}\}$. The diagonalisation of $\hat{V}(\mathcal{R})$ in the spin network basis is performed in [58]. The resulting volume spectrum is quantised. Each volume eigenvalue λ_{β_v} of a node v in $\mathcal{R}$ is labelled by β_v. Assuming that $\mathcal{R}$ contains p nodes $\{v\}$, its volume eigenvalues have the form

$$\lambda_{\underline{\beta}} = \sum_v \lambda_{\beta_v}. \tag{66}$$

The eigenvalues in (66) are the possible total volumes of all nodes in $\mathcal{R}$ and are labelled by $\underline{\beta} = \{\beta_1, \ldots, \beta_p\}$. For a node v, $\{\lambda_{\beta_v}\}$ are computed from the matrices $\{W^{n_v}_{[rts]}\}$ which are determined by the labels of the edges joined to v [58].

It is shown in [58] that 3-valent nodes have no volume. Volumes of nodes with valences 4 and 5 are tabulated in [58]. Like that of the area operator, the spectrum of the volume operator should be observable [2].

4.4 Geometry in loop quantum gravity

Having reviewed properties of spin networks and s-knots and the discrete spectra of the LQG area and volume operators, we review how these give rise to geometry in LQG. For the rest of this sub-chapter, we follow [2].

The physical interpretation of a spin network warrants elaboration. Key to this are the observations that, respectively, the actions of the area and volume operators on the spin network state $|S\rangle$ are only non-trivial on the edges and nodes of S. A quantum of spatial volume, given by λ_{β_v}, is localised on each

node and a quantum of spatial area, given by (55), is localised on each edge joining nodes. Trivalent nodes have no surrounding volume. The quanta of area are considered as being possessed by surfaces that intersect the edges and separate the quanta of volume. The volumes and surfaces are organised by the graph of $|S\rangle$. The spins and intertwiners of $|S\rangle$ are, respectively, "good quantum numbers" [8] for the area and volume. With all these ideas in mind, $|S\rangle$ is interpreted as a "metric" [2] on quantum space.

A s-knot state $|s\rangle$ can be considered a class of diffeomorphism-equivalent "metrics" [2]. Hence, $|s\rangle$ is a quantum geometry. The edges of $|s\rangle$ arrange a set of abstract and mutually localised spatial quanta. The areas and volumes of s are defined by the quantum numbers of the diffeomorphism-equivalent spin networks. Hence, s-knot states $|s\rangle$ are quantum spatial states consistent with diffeomorphism-invariance and background-independence.

$|s\rangle$ admits "regions" [2] and "surfaces" [2] that are not diffeomorphism-invariant. A set of nodes in s is a region of s. The surface enclosing the region is a set of edges that extend outside of the graph corresponding to the region. Respectively, the volumes and areas of regions and surfaces of s are defined as before.

Throughout this chapter, we have reviewed how canonical LQG quantises space. In the next chapter, we will see how LQG quantises spacetime via the covariant approach.

5 Spin foams

In this chapter, we review the covariant formulation of LQG. The covariant formulation is also called the path-integral formulation of LQG as it is a discrete analogue of that of conventional quantum field theories. While the canonical formulation could be considered mostly kinematic, the covariant formulation is mostly dynamic. The covariant formulation is inherently spacetime-covariant, background-independent and describes the dynamics of LQG as such in terms of spin foams.

5.1 The nature and origin of spin foams

Conceptually, a spin foam is a spin network with its constituents one dimension higher. Given a Lie group G, an abstract spin foam [59] is a 2D-complex, a set of 2D faces $\{f\}$ joined at 1D edges $\{e\}$ that join at nodes $\{v\}$, where each face is assigned an irrep of G labelled by j_f and each edge is assigned a G intertwiner I_e.

Spin foams have origins in the "sum over histories" (, see [63] for references,) approach to quantum systems and field theories. These ideas are manifest in the "sum over surfaces" [60, 61] and "worldsheet" [62] formulations of LQG that are also inspired by the ADM formalism. These formulations naturally lead to spin foams.

The evolution of a s-knot state [60, 61] is implemented by the Hamiltonian constraint. The evolution happens in iterations; the Hamiltonian constraint changes the number of nodes of a s-knot state between iterations. A spin foam

can be interpreted as a history of s-knot evolution under the Hamiltonian constraint. Because each s-knot of a spin foam corresponds to a hypersurface in the ADM formalism, a spin foam can be interpreted as a quantum of spacetime [61]. A "cross-section" of a spin foam is a s-knot; i.e, a "cross-section" of quantum spacetime is quantum space. Hence, the spin foam, like the spin network, has physical and abstract interpretations.

5.2 Spin foam models

A spin foam model (or model) is a construction of a covariant theory that quantises spacetime via spin foams. The generating function for a model is [2]

$$Z = \sum_{\Gamma} w(\Gamma) \sum_{j_f, I_e} \prod_{f} A_f(j_f, I_e) \prod_{e} A_e(j_f, I_e) \prod_{v} A_v(j_f, I_e) \tag{67}$$

where $\{\Gamma\}$ are 2-complexes, $\{w(\Gamma)\}$ are weights associated to $\{\Gamma\}$ and the amplitudes of the faces, edges and nodes of $\{\Gamma\}$ are denoted by $\{A_f\}$, $\{A_e\}$ and $\{A_v\}$. The canonical Hamiltonian of a theory is encoded in $\{A_v\}$ [2]. We call (67) the "master formula" (which has nothing to do with the master constraint). The master formula is the discretised path integral of a theory; $\{w(\Gamma)\}$ can thus be interpreted as a discretised measure [2]. From the perspective of [60, 61], the master formula is a sum over spin foams from and to the trivial s-knot state. In this way, models encode the sum over histories concept in [63] et. al.. A model is determined by a certain choice of parameters in the master formula [2].

A model for 4D Lorentzian GR was sought after. However, due to the theory being non-topological and the gauge Lorentz group being non-compact, it was found to be difficult to obtain the required set of parameters [2]. As a

result, simpler models, usually for compact G, were first found and studied. The generating functions of many models are special cases of the master formula [2]. For the rest of this chapter, we will review the construction and properties of certain models.

5.3 The BF model

The BF model is derived from BF theory. BF theory can be set in a spacetime of any dimension and can have any connected gauge Lie group [33]. In this sub-chapter, we set BF theory in a 4D spacetime $\mathcal{M}$ and give it the gauge group $Spin(4)$. With these choices, we will see that the BF model is a foundation for other models. For the rest of this sub-chapter, we follow [33].

First, we list some general properties of BF theory. BF theory is topological both classically and quantum mechanically. This means that it has no local degrees of freedom and any physical quantities depend only on the topology of $\mathcal{M}$. Hence, BF is always inherently background-independent. Also, 3D GR, either Euclidean or Lorentzian, is a type of BF theory. The boundary of $\mathcal{M}$, if it exists, can be the event horizon of a black hole. BF theory can be canonically quantised in a similar way as the Ashtekar formulation of 4D Lorentzian GR can; in particular, the spin network formalism is analogous.

The action of BF theory is

$$S_{BF} = \int_{\mathcal{M}} Tr(B \wedge F) \tag{68}$$

where B and F are 2-forms into $so(4)$ and F is the curvature 2-form of a

connection 1-form A. The generating function is

$$Z_{BF} = \int\int e^{iS_{BF}}\ DB\ DA = \int\int e^{i\int_{\mathcal{M}} Tr(B\wedge F)}\ DB\ DA. \tag{69}$$

The Dirac delta on the curvature 2-forms can be defined as

$$\delta(F) = \int e^{i\int_{\mathcal{M}} Tr(B\wedge F)} DB \tag{70}$$

and, hence, the B field can be integrated out to give

$$Z_{BF} = \int \delta(F)\ DA. \tag{71}$$

(71) must be discretised to have concrete meaning. This is done by using space-time triangulation, a procedure borrowed from Regge calculus [64, 65]. A triangulation Δ of $\mathcal{M}$ divides $\mathcal{M}$ into 4-simplices [66], 4D analogues of tetrahedra. To the "dual 2-skeleton" [33, 67] of each 4-simplex of Δ, orientations and elements $\{g_{ef}\} \in Spin(4)$ are assigned to the "dual edges" [33] $\{e\}$ of the "dual faces" [33] $\{f\}$. This assigns a holonomy $g_{e_1 f} \ldots g_{e_n f} \in Spin(4)$ to each dual face f with n edges. Respectively, these assignments discretise A and F on the dual 2-skeleton. The functional integral over A discretises to a product of $Spin(4)$ integrals over $\{g_{ef}\}$ with the $Spin(4)$ Haar measure. The discretisation of (71) is

$$Z_{BF} = \Big(\prod_e \int_{Spin(4)} dg_e\Big)\Big(\prod_f \delta(g_{e_1 f} \ldots g_{e_n f})\Big) \tag{72}$$

where δ is the Dirac delta on $Spin(4)$. (72) is then re-cast by substituting in the $Spin(4)$ expression of δ;

$$\delta(g) = \sum_\rho dim(\rho(g))\ Tr(\rho(g)) \tag{73}$$

where the sum is over $Spin(4)$ irreps $\{\rho\}$. This gives

$$Z_{BF} = \sum_{\rho_f} \Big(\prod_e \int_{Spin(4)} dg_e \Big) \Big(\prod_f dim(\rho_f(g_{e_1 f} \dots g_{e_n f})) Tr(\rho_f(g_{e_1 f} \dots g_{e_n f})) \Big). \tag{74}$$

Hence, $Spin(4)$ irreps $\{\rho_f\}$ are assigned to the dual faces $\{f\}$. We are getting to the language of spin foams. The $Spin(4)$ integrals are then computed using recoupling theory. The following is key; in (74), $\{\rho_f\}$ divide into sets of four and each set is assigned to a quartet of dual faces meeting at a dual edge. Given this, the $Spin(4)$ integrals of products of $\{\rho_f\}$ become sums of products of $Spin(4)$ intertwiners $\{I_e\}$ that label the dual edges. After all integrals are dispatched,

$$Z_{BF} = \sum_{j_f, I_e} \prod_f dim(\rho_{j_f}) \prod_v 15j_{Spin(4)}(\{j_f\}, \{I_e\}) \tag{75}$$

where $\{v\}$ is the set of "dual vertices" [33], we have introduced numbers $\{j_f\}$ labelling $\{\rho_f\}$ and we use the notation nj_G for the G Wigner nj symbol.

(75) is a special case of the master formula [2] as the sum over 2-complexes and the measure and edge amplitudes are trivial. A similar analysis of 3D BF theory with gauge group $SU(2)$, where triplets of $SU(2)$ irreps replace quartets of $Spin(4)$ irreps, yields the generating function of the Ponzano-Regge model [2, 68]. This reinforces the fact that 3D GR is a type of BF theory. Worryingly, (75) shows that all spin foams contribute to Z_{BF} and, thus, cause it to be infrared-divergent. However, it turns out [33] that the infrared divergence can be removed. This is done by q-deforming the BF theory, which adds a term in the cosmological constant to S_{BF}, and subsequently relating BF theory to Chern-Simons theory. The q-deformed BF model is the Crane-Yetter model

[69, 70] whose generating function is finite and independent of Δ [33, 2]. A generating function for Lorentzian BF theory with gauge group $SL(2,\mathbb{C})$ is constructed in [71].

5.4 The Barrett-Crane model

The Barrett-Crane model [72, 73] (BC model) is a constrained 4D BF model with gauge group $Spin(4)$. For the rest of this sub-chapter, we follow [74].

The BF action is modified in the following way;

$$S_{MBF}[B,A,\lambda,\mu] = \int_{\mathcal{M}} B^{IJ}\wedge F_{IJ}(A)+\lambda_{IJKL}B^{IJ}\wedge B^{KL}+\mu\epsilon^{IJKL}\lambda_{IJKL} \quad (76)$$

where $I,J,\cdots \in \{1,\ldots,4\}$ are $so(4)$ indices, ϵ^{IJKL} is the 4-index Levi-Civita symbol, λ_{IJKL} is a $so(4)$ tensor that is symmetric on the first and last pair of indices and symmetric on the pairs and μ is a 4-form. In (76), λ_{IJKL} and μ are Lagrange multipliers that enforce the following constraints:

$$\epsilon^{IJKL}\lambda_{IJKL} = 0, \quad (77)$$

$$\epsilon_{IJKL}B^{IJ}_{\mu\nu}B^{KL}_{\rho\sigma} = \tilde{e}\,\epsilon_{\mu\nu\rho\sigma} \quad (78)$$

where $\tilde{e}$ is expressed solely in terms of $B^{IJ}_{\mu\nu}$ [75]. (78) is the set of simplicity constraints. (78) is solved by a $so(4)$-valued tetradic one-form $e^I = e^I_\mu dx^\mu$ that satisfies

$$B^{IJ} = \pm\frac{1}{2}\,\epsilon^{IJ}_{KL}\,e^K\wedge e^L \quad (79)$$

[75]. There is another set of solutions to the simplicity constraints [75], (78), that are not relevant for reasons we will discuss later. Off-shell, the number of independent degrees of freedom of B is 36. On-shell, the 20 simplicity constraints

that come from λ_{IJKL} satisfying (77) lower this number to 16. Correspondingly, e^I becomes the basic field on-shell. When taken on-shell, S_{MBF} reduces to 4D Riemannian GR. Hence, imposing the simplicity constraints, (78), on the topological BF theory makes it non-topological.

Next, the constraints are discretised. The procedure for doing this starts with a triangulation Δ of $\mathcal{M}$. On either $\{f\}$ or a set of "triangles" [74] $\{t\}$, $B^{IJ}_{\mu\nu}$ is respectively discretised as a set of $so(4)$ elements $\{B^{IJ}_f\}$ or $\{B^{IJ}_t\}$. The only purpose of (77) is to ensure that the theory has the correct number of degrees of freedom on-shell. Hence, it is not necessary to analyse (77) further. To discretise (78), the triangle t can be viewed as the discrete analogy of pairs of spacetime indices $\mu\nu$. The discrete analogy of spacetime indices being repeated is that there exists a tetrahedron T that has the corresponding triangles as faces. There is a distinction between the diagonal simplicity constraints, where $t = t'$, the non-diagonal simplicity constraints, where $t, t' \in T$ and the rest called the dynamical simplicity constraints [76]. Respectively, we call these the d, n and y constraints. Upon discretisation of (78), the d and n constraints vanish but the y constraints do not;

$$\epsilon_{IJKL} B^{IJ}_t B^{KL}_{t'} \begin{cases} = 0 & t, t' \in T \\ \\ \propto \tilde{e} & \text{else} \end{cases} .$$

The d,n and y constraints can be re-cast in the equivalent form

$$C^{d,n,y}_{t\ t'}(B) := -\epsilon_{IJKL} B^{IJ}_t B^{KL}_{t'}. \tag{80}$$

The idea for defining the BC spin foam model is to impose the constraints

directly on the BF spin foam model. Central to this is an "atom" [74], an elementary region surrounding a dual vertex [33, 67]. The atom has 5 edges within it that meet at a central vertex and are assigned elements $g_p \in Spin(4)$ labelled by $p, q, \cdots \in \{1, \ldots, 5\}$. The atom also has 10 boundary edges that are assigned elements $h_{pq} = h_{qp}^{-1} \in Spin(4)$ with $p \neq q$. The amplitude of an atom of the BC model determines the BC generating function Z_{BC}. Hence, to write down Z_{BC}, only the atomic BF amplitude is required.

Given (72), the BF atomic amplitude may be simply read off;

$$A_{BF}(h_{pq}) = \prod_p \Big(\int_{Spin(4)} dg_p \Big) \Big(\prod_{p<q} \delta(g_p h_{pq} g_q) \Big) \tag{81}$$

where $\{g_p h_{pq} g_q\}$ are the holonomies of the faces that have exactly one corner as the central atomic vertex. By using re-coupling theory as in the construction of the BF model, A_{BF} can be re-expressed as

$$A_{BF}(h_{pq}) = \sum_{\rho_{pq}, I_p} \prod_{p<q} dim(\rho_{pq}) 10j_{Spin(4)} Tr'(10j_{Spin(4)}) \tag{82}$$

where $\{\rho_{pq}\}$ are $Spin(4)$ irreps, $\{I_p\}$ are $Spin(4)$ intertwiners and Tr' is the trace performed by contracting with $\{h_{pq}\}$. Moreover, it can be shown [74] that the discretised B field over $\{f\}$ can be written as

$$B_f^{IJ} = -i\chi^{IJ}(U_f) \tag{83}$$

which is a vector field of the holonomy of the face f and is left-invariant under $Spin(4)$. Given this, it is sufficient to obtain the atomic BC amplitude by sifting out the configurations that satisfy the d,n and y constraints with a functional delta;

$$A_{BC}(h_{pq}) = \delta(C^{d,n,y}(-i\chi(h_{pq})))A_{BF}(h_{pq}) \tag{84}$$

where the d,n and y constraints, in an equivalent form on the faces, are

$$C^{d,n,y}_{pqr}(-i\chi^{IJ}) = \epsilon_{IJKL}\chi^{IJ}(h_{pq})\chi^{KL}(h_{pr}). \tag{85}$$

After promoting $\{C^{d,n,y}_{pqr}\}$ to operators $\{\hat{C}^{d,n,y}_{pqr}\}$, the quantised d and n constraints are imposed on the atomic BC amplitude as

$$\hat{C}^{d,n}_{pqr}A_{BC}(h_{pq}) = \epsilon_{IJKL}\chi^{IJ}(h_{pq})\chi^{KL}(h_{pr})A_{BC}(h_{pq}) = 0 \;\forall q, r \tag{86}$$

for fixed p. These constraints are second-class [77, 26]. The gauge-invariance constraint from the BF theory [33], which is expressed post-triangulation as

$$\sum_{t\in T} B^{IJ}_t = 0 \quad \forall\, T, \tag{87}$$

means that there are 20 independent constraints as required by (77) and (78). It can be shown [74] that, up to a factor, a unique solution to all constraints, including the second-class dynamical ones, is

$$A_{BC}(h_{pq}) = \sum_{j_{pq}, I_p} \prod_{p<q} \dim(\rho_{pq}) 10j^{BC}_{Spin(4)} Tr'(10j^{BC}_{Spin(4)}). \tag{88}$$

Due to the d constraints and $Spin(4) \simeq SU(2)\otimes SU(2)$, $\rho_{pq} = j_{pq}\otimes j^*_{pq}$ are simple [77]. Also, j is an irrep of $SU(2)$, j^* is its dual and $10j^{BC}_{Spin(4)}$ is $10j_{Spin(4)}$ with the vertex $Spin(4)$ intertwiners replaced by Barrett-Crane intertwiners [72]. The Barrett-Crane intertwiner can be defined [78] as the unique, up to a factor, $Spin(4)$ (0,4) intertwiner of the "relativistic spin networks" [72] that solves all constraints. Hence, the constraints are imposed on the atomic BF amplitude by replacing the intertwiners. From this, the BC generating function is the sum of all given contributions from the atomic BC amplitudes;

$$Z_{BC} = \sum_{j_f} \prod_f dim(\rho_{j_f}) \prod_e A_e \prod_v 10j^{BC}_{Spin(4)} \tag{89}$$

where $\{j_f\}$ label simple $\{\rho_{pq}\}$ and $\{A_e\}$ are arbitrary edge amplitudes. There are additional simple $\{\rho_{pq}\}$ corresponding to the extra solutions to the simplicity constraints, (78), but these do not contribute to Z_{BC} (; see [74] and references therein). (89) is a special case of the master formula [2] as the sum over 2-complexes, measure and sum over intertwiners are trivial.

The BC model has 4D Riemannian GR as a semiclassical limit (; see [74] and references therein). Also, it can be shown [72], via q-deformation, that the BC model is finite. The area spectrum of $\{t\}$ is discrete and is the same as the LQG area spectrum. However, there is no well-defined volume operator. Also, the space of boundary s-knots of the BC spin foams is not the same as the s-knot space of LQG with gauge group $SO(3)$ [77]. We say that the BC model is not covariant to $SO(3)$ LQG. The Lorentzian BC model is proposed in [73]. It is shown in [79] that this model is finite. In the next sub-chapter, we will review a model that resolves the issues of the BC model.

5.5 The EPRL model

The problems that prevent the Riemannian BC model from being covariant to LQG originate from the fact that the n constraints are strongly imposed [77]. In fact, the constraints are so strong that any intertwiner other than the BC intertwiner is forbidden. This fixes the intertwiner degrees of freedom which, because the constraints are second-class, means that there are fewer physical degrees of freedom than there should be [77]. In [77, 80], an improvement of the Riemannian BC model is proposed. The two models are very similar; the

only differences are their allowed intertwiners. While the BC model restricts to the BC intertwiner, the proposed model allows a subspace of all $SO(4)$ (0,4) intertwiners. Hence, the n constraints are imposed weakly in this subspace [77]. This preserves the intertwiner degrees of freedom so that the proposed model has the right number of physical degrees of freedom. Because of this, the proposed model is covariant to $SO(3)$ LQG. In [81], Pereira constructs the Lorentzian variant of the model which, like the Riemannian model, retains all physical degrees of freedom. This means that the model is covariant to $SU(2)$ LQG. In [76], the Riemannian and Lorentzian models are generalised to any finite value of γ. The resulting generating function for the Riemannian model is

$$Z^E = \sum_{j_f, I_e} \prod_f d_f^E(\gamma) \prod_v A^E(\gamma, j_f, I_e) \tag{90}$$

and that for the Lorentzian model is

$$Z^L = \sum_{j_f, I_e} \prod_f d_f^L(\gamma) \prod_v A^L(\gamma, j_f, I_e) \tag{91}$$

where $d_f^E(\gamma) = (|1-\gamma| j_f + 1)((1+\gamma) j_f + 1)$ and $d_f^L(\gamma) = (2j_f)^2(1+\gamma^2)$ and the vertex amplitudes $A^E(\gamma, j_f, I_e)$ and $A^L(\gamma, j_f, I_e)$ are given in [76] in terms of, respectively, $SU(2)$ and $SL(2,\mathbb{C})$ Wigner $15j$ symbols. Respectively, these generating functions reduce to those in [77, 80] and [81] for $\gamma = 0$. In (90) and (91), the measure and edge amplitudes are trivial. Since the face and vertex amplitudes are also functions of γ, (90) and (91) can be viewed as extensions of the master formula. We call the models with generating functions Z^E and Z^L, respectively, the Riemannian and Lorentzian EPRL models. In [82], it is shown

that the Lorentzian EPRL model is finite. Both EPRL models are covariant to $SU(2)$ LQG for all γ and have the LQG area spectrum [76]. Remarkably, the Riemannian and Lorentzian EPRL models, respectively, have 4D Riemannian and Lorentzian GR as semiclassical limits [83, 84, 85]. Hence, the Lorentzian EPRL model is of particular interest for being physically accurate.

5.6 The spin foam - GFT correspondence

Each model can be constructed in terms of a group field theory (GFT) (; see [76] and references therein). A GFT [86] over a group G is a theory of a field $\phi : G^D \rightarrow \mathbb{C}$. The GFT configuration space is thus G group multiplied by itself D times. The momentum space is determined by the configuration space through harmonic analysis; this gives an analogue of the Fourier transform of ϕ. ϕ is the analogue of a "scalar field" of a Poincarè-invariant scalar field theory; the analogue of Lorentz symmetry is the right invariance of ϕ under G;

$$\phi(\{g_I g\}_{I=1}^D) = \phi(\{g_I\}_{I=1}^D) \quad \forall\, g \in G. \tag{92}$$

The GFT action $S_D[\phi]$ has this as a global symmetry. The form of the GFT action is given in [86] and is the sum of a kinetic term and a non-local self-interaction term with interaction strength λ.

The GFT generating function is

$$Z = \int e^{-S_D[\phi]} D\phi \tag{93}$$

which has the following perturbative expansion;

$$Z = \sum_{\Gamma} \frac{\lambda^{n(\Gamma)}}{Sym(\Gamma)} Z(\Gamma) \tag{94}$$

where $\{\Gamma\}$ are 2D Feynman graphs and $n(\Gamma)$, $Sym(\Gamma)$ and $Z(\Gamma)$ are, respectively, the number of vertices, symmetry factor and amplitude of Γ. The correspondence is the following [86]; each GFT generating function is a spin-foam generating function where each Γ is a spin foam with amplitude

$$Z(\Gamma) = \sum_{j_f, I_e} \prod_f A_f(j_f, I_e) \prod_e A_e(j_f, I_e) \prod_v A_v(j_f, I_e). \tag{95}$$

This works because substituting (95) into (94) yields the master formula, (67), with measure $\frac{\lambda^{n(\Gamma)}}{Sym(\Gamma)}$. The GFT corresponding to a model is unique [74]. Understanding of a model can be gained by analysis of its "dual" GFT; this is how finiteness and triangulation independence may be shown [74]. The GFT method is used in [74] to analyse the Riemannian and Lorentzian BC models and fix their edge amplitudes.

This chapter shows that there are interesting similarities between LQG and string theory [87]. The "sum over surfaces" [60, 61] or sum over "worldsheets" [62] is precisely analogous to that in string theory [60]. Also, both types of theories can be dual to quantum field theories. We will further discuss this relation in sub-chapter 7.5.

6 Applications to black holes

In this chapter, we will review applications of some results from LQG to the entropy of black holes and Hawking radiation. These will show that LQG is now able to explain real-world phenomena but the explanations of these it provides are not yet complete.

6.1 Black hole entropy

Bekenstein [15] and Hawking [16] showed that the entropy of a black hole is

$$S_{BH} = 2\pi A \tag{96}$$

where A is the area of the event horizon. This is the Bekenstein-Hawking (BH) entropy. It is a semiclassical property of the black hole horizon. The BH entropy has been derived within LQG [88] by considering intersections between spin network edges and the quantised horizon and treating microstates of the horizon as those of a $U(1)$ Chern-Simons theory. For the rest of this sub-chapter, we follow a simpler derivation from [14] which uses statistical mechanics [89] and combines results from LQG with semi-classical ideas about the horizon.

Consider a Schwarzschild black hole in thermal equilibrium with a reservoir. Let the reservoir include an observer outside and near the horizon with uniform acceleration a that matches the surface gravity at their position. Also, let the reservoir be at the Unruh temperature [90]

$$T_U = \frac{a}{2\pi}. \tag{97}$$

Information from the black hole interior is forbidden from reaching the exterior vacuum spacetime and the horizon. Thus, all the observer sees is the horizon which appears to be a 2D spatial surface whose time evolution only depends on the exterior spacetime. It can be shown [91] that the thermodynamic energy of the horizon with respect to the observer is

$$E_H = Aa. \tag{98}$$

The semi-classical horizon would be a perfect sphere in thermal equilibrium but deforms due to random thermal fluctuations that change its shape and area. Hence, the semi-classical horizon is expected to be governed by statistical mechanics [89]. By (98), changes in the horizon area cause changes of the horizon energy via energy transfer between the black hole and the reservoir. Hence, the horizon is best treated in the canonical ensemble [89]. From the view of LQG, quanta of space surround the horizon. It is assumed that one spin network edge of each spatial quantum intersects the horizon. Via the non-degenerate area spectrum in (56), an intersection of the horizon and a spin-j edge has associated area

$$A_j = \gamma\sqrt{j(j+1)}. \tag{99}$$

The degenerate sector has no relevance in this discussion. We consider an intersection as a system in equilibrium with the reservoir. We consider a macrostate [89] of the system as a set of microstates [89] with the same spin j and same corresponding energy E_j as measured by the observer. Explicitly, E_j is E_H with

area $A = A_j$; i.e,

$$E_j = A_j a = a\gamma\sqrt{j(j+1)}. \tag{100}$$

A spin-j macrostate has microstates labelled by j and $m \in \{-j, -(j-1), \ldots, j-1, j\}$ [54] so the macrostate has a multiplicity of $2j+1$. The finiteness of the macrostate multiplices is due to quantum geometry in LQG and ensures that the problem of finding the black hole entropy is well-posed. The system macrostate with spin j and energy E_j has probability [89] proportional to the multiplicity weighted with a Boltzmann factor;

$$p_j(\beta) \propto (2j+1)e^{-\beta E_j} \tag{101}$$

where $\beta = \frac{1}{T_U}$. Then, (100) is substituted into (101) to give

$$p_j(\beta) \propto (2j+1)e^{-\beta a\gamma\sqrt{j(j+1)}}. \tag{102}$$

We write (102) as an equality;

$$p_j(\beta) = Z(\beta)^{-1}(2j+1)e^{-\beta a\gamma\sqrt{j(j+1)}} \tag{103}$$

where $Z(\beta)$ is the partition function of the system. The macrostate probabilities $\{p_j\}$ are normalised; substituting (103) into the normalisation condition yields

$$Z(\beta) = \sum_j (2j+1)e^{-\beta a\gamma\sqrt{j(j+1)}}. \tag{104}$$

As the system is in the canonical ensemble [89], its thermodynamic quantities are related by

$$-T_U ln(Z) = E_H - T_U S \tag{105}$$

where the semi-classical average energy is E_H and

$$S = -\sum_j p_j ln(p_j) \tag{106}$$

is the Gibbs entropy [89]. Re-arranging (105) gives

$$S = \frac{E_H}{T_U} + \ ln(Z). \tag{107}$$

(97), (98) and (104) are substituted into (107) to give

$$S = 2\pi A + \ ln \sum_j (2j+1) e^{-2\pi\gamma\sqrt{j(j+1)}}. \tag{108}$$

The statement that $S = S_{BH}$ holds iff

$$\sum_j (2j+1) e^{-2\pi\gamma\sqrt{j(j+1)}} = 1. \tag{109}$$

The numerical solution of (109) is

$$\gamma = \gamma_0 = 0.274. \tag{110}$$

Hence, this analysis shows that the LQG-inspired entropy matches the BH entropy iff $\gamma = \gamma_0$ is a numerical constant that solves (109). It is possible to account for the degenerate sector; this was done by Krasnov [92]. Krasnov obtained the entropy $S_K = \alpha_c A$ where α_c is inversely proportional to γ. This linearly relates entropy and horizon area as the BH entropy in (96) does. However, the analysis of Krasnov [92] does not fix γ and so does not fix α_c.

A calculation of the Schwarzschild black hole entropy with an arbitrary number of horizon-edge intersections per spatial state is performed in [93, 18]. We informally motivate the result of [93, 18] by using concepts from the analysis of

[14] we reviewed earlier in this sub-chapter. The condition for $S = S_{BH}$,

$$ln \sum_j (2j+1) e^{-2\pi\gamma\sqrt{j(j+1)}} = 0, \tag{111}$$

states that the total entropy of the intersections is zero [88, 18]. Upon relaxing this condition, the left-hand side of (111) becomes a function of γ denoted by $\sigma(\gamma)$ [93, 18]. We interpret $\sigma(\gamma)$ as the entropy of the intersections at Immirzi parameter γ. If all spatial states are allowed to have the same number of intersections N, the total entropy of all intersections is $S_I(\gamma) = \sigma(\gamma)N$. Hence, the total entropy of the black hole is

$$S_T(\gamma) = S_{BH} + S_I(\gamma). \tag{112}$$

The overall horizon gives a semi-classical entropy contribution S_{BH} and all intersections give a total quantum geometrical contribution S_I that varies with γ [93, 18]. This reinforces that the value of γ matters in the quantum theory. Currently, neither S_K nor S_T can be fixed as the LQG literature disagrees on the value of γ.

6.2 Hawking radiation

Hawking predicts [16, 17] that a black hole has the thermodynamic behaviour of a black body with a corresponding emission spectrum and a temperature

$$T_H = \frac{\kappa}{2\pi} \tag{113}$$

where κ is the black hole surface gravity. In place of a rigorous analysis of Hawking radiation within LQG [18], interim frameworks have been proposed.

Before the LQG area operator was analysed, Bekenstein [94] and Mukhanov [95] made the quantum geometrical assumption that the area of a black hole horizon is quantised as

$$A_n = \alpha n \tag{114}$$

where $\alpha > 0$ [96, 97]. We call this the Bekenstein-Muhkanov (BM) quantisation. It can be shown [96, 97] that this leads to the black hole having a discrete set of energy levels. In this way, the black hole is thermodynamically analogous to an atom with respect to the energy level structure and level transitions. For a macroscopic black hole, the spacing between consecutive levels should be constant at ω where ω is the associated frequency and inversely proportional to the black hole mass [96, 97]. Hence, an arbitrary de-excitation should result in the emission of energy equal to a natural number times ω [96, 97] and thus a corresponding line on the emission spectrum. Indeed, lines associated to single-quantum emission appear at natural number multiples of frequency ω with the line at ω corresponding to the level spacing [96, 97]. However, the emission frequencies may vary due to quantum fluctuations [3]; this may cause lines to appear elsewhere on the spectrum, including before ω [96]. The spectrum appears as a set of "smudges" and may be further smeared by multi-quanta emissions [96]. Nonetheless, [96] argues that the smudges are distinct. Further, it is shown [96] that their intensity decreases exponentially with frequency so

[3] Additionally, Hawking radiation gradually reduces the black hole mass and thus increases ω. Neglecting quantum fluctuations, this makes consecutive levels gradually separate. However, the weakness of Hawking radiation makes this happen extremely slowly. For analysing the spectrum, a constant black hole mass is a very good approximation.

the lowest frequency line at ω should be brightest. Hence, the spectrum of line intensities differs from the spectrum predicted by Hawking [16, 17] in that the BM spectrum is discrete and predicts a different intensity of the lowest frequency line. The findings of the BM quantisation support a discrete black hole spectrum but are inconclusive.

Another analysis of the black hole spectrum was conducted by Krasnov [98]. Krasnov analyses the spectrum by treating edge-horizon intersections, as seen in the previous sub-chapter, as "atoms" [98]. An atom is analogous to an atom of matter where the spin j replaces the energy as a level quantum number. Atomic transitions between levels of given spins produce lines on the emission spectrum. Krasnov expects multi-atom transitions to be suppressed and some transitions to be forbidden by selection rules. Hence, from a possibly more complete spectrum, Krasnov isolates the dominant spectral lines due to 1-atom transitions [98]. Krasnov uses Fermi's golden rule [1] to compute the atomic line intensities [98] as can be done for the spectra of atoms of matter. This is achieved in a variant of the canonical ensemble where area replaces energy [98]. The resulting spectrum [98] approximates a discrete black body spectrum. Hence, the BM and Krasnov spectral intensities are different at small frequencies and, thus, for the lowest frequency line [98]. As the analysis of Krasnov [98] discounts quantum fluctuations and multi-atom transitions, it is insufficient to determine whether the black hole spectrum is continuous or discrete.

A possible resolution to this ambiguity was proposed in [97]. In [97], the macroscopic black hole horizon assumes the non-degenerate LQG area spec-

trum. It is shown [97] that the emission spectrum of such a black hole is effectively continuous. This suggests that LQG agrees with the continuous spectrum predicted by Hawking [16, 17] in the macroscopic case. Consequently, LQG is incompatible with the BM quantisation but the latter may be correct regardless of whether LQG is and may be useful for microscopic black holes.

An analysis of spherical black hole radiation within LQG is presented in [99]. In [99], it is shown that the expected number of emitted scalar particles is the sum of the Hawking result [16, 17] and a quantum correction that is small for macroscopic black holes. From this, it might be expected that the Hawking temperature (113) would be corrected accordingly.

To conclude this sub-chapter, we note that Monte-Carlo simulations of Hawking radiation using LQG have been performed in [100, 101]. Certain features of the computed spectra [100, 101] arise due to LQG and can be identified. Hence, if Hawking radiation could be observed, LQG could be tested by checking the black hole spectra for these features. However, [100, 101] have different levels of optimism for this method.

7 Current topics

In this chapter, we review some direct and indirect applications and areas of LQG that have been developed within the last few years. Some of these could help to address certain problems with LQG or spawn entirely new relations between LQG and other areas of physics.

7.1 Fractal horizons

Recently, Barrow [102] proposed the elegant idea (, loosely inspired by the COVID-19 pandemic,) that the structure of the Schwarzschild black hole horizon is fractal to the Planck scale. The resulting "fractal black hole" [102] is a possible artefact of quantum gravity. We give a review of this idea in this sub-chapter.

Barrow constructs the fractal horizon by iterating an ordinary Schwarzschild horizon à la the Koch snowflake [103] with spheres replacing triangles. Barrow requests, for consistency with fractal geometry (, see [102] and references therein,), that

$$\lambda^{-2} < N < \lambda^{-3} \tag{115}$$

where, between iterations, N is the number of spheres added to each sphere and λ is the radius scale factor. Since each sphere has a finite size, Barrow expects an upper-bound on N that is stricter than (115). Compared to the ordinary Schwarzschild black hole, the fractal black hole has a far larger horizon area, a far larger entropy and a smaller lifetime [102]. Barrow quantifies how fractal the horizon is with a parameter $\Delta \in [0, 1]$ that encodes the Hausdorff dimension

[104] $D \in [2,3]$ of the horizon. In the extreme cases, $\Delta = 0$ gives the ordinary Schwarzschild horizon with $D = 2$ and $\Delta = 1$ gives a perfect fractal with $D = 3$ [102]. Barrow estimates the fractal black hole entropy as

$$S_F \approx \Big(\frac{A}{A_p}\Big)^{\frac{2+\Delta}{2}} \tag{116}$$

where A is the area of the horizon and A_p is the Planck area. The range of S_F is very large [102] and includes the BH entropy, (96), for $\Delta = 0$.

The origins of the fractal black hole [102] include the covariant LQG formulation; it is assumed that the complicated structure of quantum spacetime therein carries over to the black hole in the form of a fractal horizon. Unfortunately, the fractal black hole is shown to not be stable in [105]. Nevertheless, [106] shows that, within LQG, replacing the Gibbs entropy with the fractal black hole entropy makes γ and the minimum spin vary with Δ. Consequences of fractal black hole entropy for thermodynamics and cosmology can be found in [107] and references in [102].

7.2 Quantum-corrected black hole

An alternative conclusion for a black hole was recently proposed in [108]. Instead of evaporating or exploding, a black hole may become a white hole via quantum tunnelling. This relies on modifying a black/white hole metric [108] with quantum corrections and is a possible solution to the information loss paradox. Many variations of the idea of [108] have been proposed within LQG and other contexts (; see [19] for references). In this sub-chapter, we focus on a quantum-corrected Schwarzschild black hole within LQG that was recently

constructed in [109, 19]. This is suitable to describe with the concepts we have reviewed in this dissertation. Only macroscopic black holes are considered as the method relies on an effective LQG description that only applies to them [109, 19]. In our description of the black hole in [109, 19], we follow [19].

The set-up of the classical maximally-extended Schwarzschild spacetime [19] employs a spherically symmetric adaptation of the Ashtekar formulation of GR. However, there are formal differences in the exterior region. This is because the Schwarzschild coordinates t and r swap over there. Hence, the exterior is foliated à la ADM by 3D timelike hypersurfaces parameterised by r. These are Lorentzian, as is the internal space in the exterior, so the gauge group is $SU(1,1)$ there.

The effective spacetime [19] is formulated by perturbing the classical spacetime with quantum corrections quantified by the parameters δ_b and δ_c. These are chosen to be functions of the area gap Δ and approach 0 in the classical limit where $\Delta \to 0$. Instead of the Schwarzschild singularity in the classical spacetime, the interior effective spacetime has a transition surface $\mathcal{T}$ that is regular and approaches the Schwarzschild singularity in the classical limit. To the past of $\mathcal{T}$, there is a "trapped region" [19] where the trajectories cannot exit and which has a past boundary with respect to $\mathcal{T}$. To the future of $\mathcal{T}$, there is an "anti-trapped region" [19] where the trajectories must exit and which has a future boundary with respect to $\mathcal{T}$. It is important to note that the trapped and anti-trapped regions are regular. However, they may be respectively interpreted as black and white hole interiors that are modified so as to be singularity-free.

Correspondingly, with respect to $\mathcal{T}$, the past and future boundaries are respectively interpreted as black and white hole horizons. In this sub-chapter, where we refer to black and white hole interiors, we refer to their regular modifications.

It is shown [19] that, wherever the black hole and white hole interiors and the exterior spacetime join to each other, they do so continuously. They form an effective spacetime region consisting of the exterior asymptotic region and an interior region that is the union of a black hole interior and a white hole interior. However, the effective spacetime region is not the full spacetime. The spacetime is maximally extended in [19]. The maximally-extended effective spacetime consists of an infinite number of asymptotic regions joined continuously to an infinite number of regions where transition surfaces separate black and white hole interiors. Correspondingly, the full effective spacetime has an infinite Penrose diagram. It is shown [19] that the full effective spacetime is completely regular everywhere.

Further consequences of the quantum corrections δ_b and δ_c are corrections to the Einstein tensor G_{ab} and upper bounds on curvature-invariants near $\mathcal{T}$ that do not depend on the black hole mass and are inversely proportional to Δ^3. Quantum geometry fundamentally causes both consequences. Numerical analysis of the curvature-invariants and induced energy-momentum stress tensor shows that the quantum corrections have large magnitudes near $\mathcal{T}$. This is such that the classical Schwarzschild interior is sufficiently modified to eliminate the Schwarzschild singularity. Further, the numerical analysis shows that the corrections are negligible near the horizons and in the asymptotic region. Hence,

it is predicted [109, 19] that the quantum corrections only significantly change the classical Schwarzchild spacetime in the interior region.

Further work has been done on this quantum-corrected black hole. Properties such as its Hawking temperature and asymptotic flatness are studied in [110]. Properties of radial geodesics are studied in [111]. From the radial geodesics, it is found [111] that the physics of the black hole are significantly different close to the horizon and in the asymptotic region than expected. It is argued [111] that this conflicts with the finding in [109, 19] that the quantum corrections do not significantly affect the classical asymptotic spacetime.

7.3 A model for Hawking radiation

Recently, a model for Hawking radiation from a spherical macroscopic black hole was proposed in [112]. We give a brief overview of this and follow [112] in this sub-chapter. As with the black hole entropy analysis of [14], the analysis of [112] treats the black hole within LQG but with semi-classical input. The analysis exploits the duality between the black hole horizon and Chern-Simons theory (; see [112] and references therein). This is used to define the "fluid approximation" [112] in which microstates of the horizon, which are intertwiners by duality, are treated as elements of a fluid. The elements are called "puncels" [112] which associate to spin network vertices connecting edges of large spin. The analysis is subsequently restricted to a certain set of states [112].

Next, the black hole is Wick-rotated to a Euclidean black hole. Classically, the Wick-rotated black hole interior is a spherical ball and the Wick-rotated

horizon is the boundary 2-sphere. For the rest of this sub-chapter, when we say "black hole", we refer to the Euclidean type. After the Wick rotation, the black hole is partitioned into puncels. A volume operator is assigned to the black hole and the volume spectrum of the puncels is computed. However, [112] infers that quantum fluctuations of the black hole volume can occur via changes in puncel number. These arise from local and small-magnitude quantum fluctuations in the radius and shape of the black hole and its horizon. [112] deduces that these give rise to a semi-classical behaviour of the horizon where it is a 2-sphere with local quantum defects. Further, [112] induces that the defects on the horizon are small in number but line up with each other and are separated by an arc length $\lambda \sim \sqrt{a_H}$ where a_H is the horizon area. Two analogies of this are posed in [112]: use of particle scattering to resolve defect spacings comparable with the de Broglie wavelength λ and a standing wave on the horizon of wavelength λ and whose antinodes are defects.

We provide a brief derivation of the result in [112] for the temperature T of the black hole. For a Schwarzschild black hole,

$$a_H \propto M^2 \tag{117}$$

where M is the black hole mass. By analogy with classical thermodynamics and the Planck energy quantisation, the energy E and temperature of the black hole might be expected to semi-classically relate via

$$E = T = \frac{2\pi}{\lambda}. \tag{118}$$

Via (117), we have

$$T \sim \frac{2\pi}{M} \sim \frac{1}{M}. \tag{119}$$

This is the result of [112]. For the Schwarzschild black hole, we have $\kappa = \frac{2\pi}{M}$ so (113) becomes

$$T_H = \frac{1}{M}. \tag{120}$$

Hence, [112] recovers the Hawking temperature up to an undetermined factor. It would be interesting to see whether the black hole could be Wick-rotated back to a conventional Lorentzian black hole and, hence, how the results of [112] would apply, if at all.

7.4 Effective spin-foam models

It has been found that models may suffer from the "flatness problem" (; see [113] and references therein). This makes the models either have undesirable properties or be incompatible with GR. A solution to this problem was recently proposed in [114] via the introduction of effective 4D Euclidean models. We briefly review these here; we follow [114] for the rest of this sub-chapter. [114] starts by applying a triangulation Δ to spacetime. The non-degenerate asymptotic form of the LQG area spectrum is assumed;

$$a_j = \gamma\sqrt{j(j+1)} \sim \gamma(j+\frac{1}{2}) \; as \; j \to \infty. \tag{121}$$

This is the possible set of areas possessed by triangles $\{t\}$ of 4-simplices of Δ. The Euclidean GR action is triangulated à la Regge [64]. However, [114] deviates from the original Regge formulation of GR [64] by expressing the action

in terms of the areas $\{a_t\}$ of $\{t\}$ rather than the lengths. The analogy of tetrahedra joining at triangular faces, one dimension higher, is 4-simplices of Δ meeting at tetrahedra. To ensure that the 4-simplices join together in a way that is consistent with the original Regge formulation, constraints are imposed on $\{a_t\}$. The constraints are implemented by $G_\tau^{\sigma,\sigma'}(\{j_t\})$, a function of the spins $\{j_t\}$ of $\{t\}$ that is labelled by the tetrahedron τ joining the 4-simplices σ and σ'. In the language of P.A.M Dirac [26], the constraints are second-class. The generating function of the effective models is

$$Z_{eff} = \sum_{j_t} \mu(j_t) \prod_t A_t(j_t) \prod_\sigma A_\sigma(j_t) \prod_\tau G_\tau^{\sigma,\sigma'}(j_t) \tag{122}$$

where $\mu(j)$ is a measure and expressions for the triangle amplitudes $A_t(\{j\})$ and 4-simplex amplitudes $A_\sigma(\{j\})$ are given in [114]. With the chosen area spectrum, the constraints are strong if imposed via making $G_\tau^{\sigma,\sigma'}$ a Heaviside function. In this case, as the constraints are second-class, they remove physical degrees of freedom as with the EPRL models. This problem is resolved by implementing the constraints weakly in a way made precise in [114]. It is proposed [114] that the constraints $G_\tau^{\sigma,\sigma'}$ modify the Riemannian BC model such that the effective model is covariant to LQG. In this case, (122) can be viewed as extending the master formula, (67). Alternatively, it is proposed [114] that the Riemannian EPRL model is the large-spin limit of the effective model. The solution to the flatness problem provided by the effective model constrains γ according to the spin and geometry of a simple triangulation [114]. A notable application for these effective models is using them to study the emergence of GR from LQG [114].

7.5 LQG and string theory

LQG and string theory [87] are candidates for quantum gravity. However, they have opposite views on spacetime. LQG is background-independent while string theory is background-dependent. Also, LQG quantises spacetime whereas the embedding spacetime for a string worldsheet is classical. Moreover, both theories give different perspectives on quantum gravity. String theory gives a view from particle physics as it predicts the graviton as the quantum of the gravitational field [87] whereas LQG gives a view from GR as it predicts the spin foam as the quantum of spacetime. Despite their differences, a unification of the two theories was recently proposed in [115]. This was based on a construction of the Nambu-Goto action [87] from the LQG area operator and results in the string tension being γ up to a factor [115]. Also, it was recently shown [116] that, upon discretising GR [116], it is possible to have spin networks whose edges are replaced by "cosmic strings" [116]. Further, it can be shown (, see [116] and references therein,) that excitations of spin network edges may correspond to particles like how particles are excitations of strings. These proposals, along with the similarities pointed out in sub-chapter 5.6, hint at either a unified theory of LQG and string theory [115] or a duality between the two. The author highly anticipates to see if either of these is the case.

8 Conclusion

In this dissertation, we have reviewed aspects of LQG. Firstly, we reviewed the Ashtekar formulation of GR in terms of a constrained Yang-Mills theory. Then, we reviewed several quantisation procedures, including canonical quantisation. Then, we reviewed elements of the canonical quantum theory including quantum geometry and that the area and volume operators have discrete eigenspectra. Then, we reviewed the covariant spin-foam formulation of LQG and its various models. Then, we reviewed applications of LQG to black holes, including a recovery of the BH entropy from the area spectrum and models for Hawking radiation. Finally, we reviewed topics on black holes, spin foams and unification that have been recently approached with LQG.

We now briefly review other achievements of LQG that we have and have not covered in this dissertation. LQG is a successful unification of GR and QM which is non-perturbative and background-independent, the latter of which is a good sign for a true theory of quantum gravity. Another good sign is that topology change is permitted in LQG; indeed, nothing about the topology of any abstract manifold in the quantum theory had to be assumed (; see [6] and references therein). Quantum space and quantum spacetime are constructed in terms of, respectively, s-knots and spin foams. The eigenspectra of the area and volume operators are physical predictions of LQG and are theoretically observable [2]. The dynamics of LQG are encoded in the Hamiltonian constraint via the canonical formulation and spin foams via the covariant formulation. Because LQG with matter from the SM has a finite Hamiltonian [2, 6], coupling

LQG to matter is possible and well-defined. The Lorentzian EPRL model is the most promising output of the covariant formulation as it is finite [82] and consistent with 4D Lorentzian GR [83, 84, 85]. Quantum-corrected LQG black holes are regular everywhere (; see [19] and references therein). LQC and spin-foam cosmology have been formulated and have the correct semi-classical limits [2, 14]. LQC eliminates singularities in universal evolution and provides an alternative bounce-inflation universal beginning and narrows down universal endings (; see [11, 12] and references therein). n-point functions and amplitudes, including the graviton propagator, have been computed in LQG (; see [14] and references therein). To conclude this paragraph, particles may arise naturally in LQG (; see [116] and references therein).

However, LQG has shortcomings that require further research. Firstly, there is no experimental evidence for or against LQG. This is because it has not been possible to acquire evidence due to difficulties in directly probing the Planck scale. Direct tests might come from Hawking radiation [20] and features of black hole spectra [100, 101]. Also, an explanation of how Hawking radiation arises from LQG may be used in tandem with these to provide precision tests for LQG. However, Hawking radiation is too weak to be observed with current methods.

The definitions of certain operators in LQG are ambiguous. There are many candidates for the Hamiltonian operator due to its various forms and regularisations [45, 46, 47]. As a result, there is no agreement on the correct Hamiltonian operator [2]. Correspondingly, there is no agreement on the correct physical

Hilbert space [34]. Also, there are different ways of constructing and regularising the area and volume operators. In [2], it is suggested that only the non-degenerate spectrum is physical and that the degenerate area eigenvalues can be removed via regularisation [2]. Experimental results may be needed to determine which operator expressions are correct [2].

The relation between the canonical and covariant formulations of LQG is not fully established. They have been proved equivalent in 3D [117] but the 4D case is an open problem. It is also open as to whether the canonical formulation semi-classically recovers GR. There are conflicting views on this. For example, n-point functions provide evidence for this (; see [14] and references therein). However, black hole entropy corrections provide evidence against this [118, 119]. Fully establishing the equivalence of both formulations may resolve the problem.

The quantum theory is ambiguous in that some of its observable predictions depend on γ. To make matters worse, there is a disagreement among the LQG literature on the value of γ. Despite the difficulties, it may be necessary to experimentally determine γ, possibly by way of measuring Δ. Even then, γ may be complex, in which case it may be worth investigating whether Ashtekar's choice $\gamma = \pm i$ [27, 28] has any physical significance.

Certain modifications of LQG warrant further study. These include LQG with matter, q-deformed LQG and spin-foam cosmology [14].

Recently, it has been proposed that a high-mass star becomes an intermediate object between gravitational collapse and black hole formation, a "Planck star" [120]. [14] has asked whether LQG can be used to analyse this object.

We conclude the areas for further research with phenomenological problems. While the classical theory has local Lorentz symmetry, there is a debate about whether the symmetry exists in the quantum theory. Consequences of breaking Lorentz symmetry are explanations of the observations of ultra-high-energy cosmic rays and TeV photons [121]. Further consequences are changes to energy-momentum and dispersion relations of particles [20]. It has been proposed [20] that the latter is related to LQG. The "modified dispersion relation" [20] causes photonic bi-refringence and is among other photonic properties expected to be modified by LQG [20]. Phenomenological tests for LQC come from modifications it makes to universal inflation [21] and properties of the cosmic microwave background [20, 21]. A solution to the trans-Planckian problem in LQC may explain apparent discrepancies between the theoretical and observed CMB power spectra [21]. Also, if the proposed black-to-white hole tunneling [108] exists, it would provide mechanisms for how fast radio bursts and the galactic central gamma-ray excess occur [21]. However, LQG phenomenological predictions are generally difficult to observe, have not been observed and may support other theories of quantum gravity instead [20]. Nevertheless, LQG phenomenology, including new models and ways to test them, is closing the gap between theory and observation, albeit very slowly.

We conclude this dissertation with the author's overall opinion. LQG is a novel and interesting theory. It combines its own concepts with those from other programs such as group field theory [86], the Wheeler-DeWitt equation [42], Regge calculus [64] and string theory [87] in a unique attempt at quantum

gravity. However, experiments will be needed to fix ambiguities in LQG and test it. The problem with this is that such experiments may remain theoretical for a long time. Even if they are eventually performed, they may agree with other existing quantum gravity theories or none at all. The latter case is especially troubling. The correct theory of quantum gravity could be something completely unrelated to any known theories; this is also suggested in [4]. This theory may be so complex that it can only be understood by artificial intelligence. For now, the author patiently anticipates learning whether LQG is the correct theory of quantum gravity.

9 Acknowledgements and references

The author wishes to thank Professor João Magueijo for his design of a project tailored to the interests of the author and for his guidance and advice on this dissertation. The author thanks Professor Andrew Tolley for generally supervising the author and for completing many university references. The author thanks Professor Andrew Green of University College London for his advice and references. Finally, the author wishes to thank Dr William Dunn of University College London for his support and encouragement.

References

[1] Bransden B Joachain C 2000 *Quantum Mechanics* (Harlow: Pearson Education Limited)

[2] Rovelli C 2004 *Quantum Gravity* Landshoff Nelson Weinberg (Cambridge: Cambridge University Press)

[3] Wald R 1984 *General Relativity* (Chicago: The University of Chicago Press)

[4] Donoghue J 1997 Perturbative dynamics of quantum general relativity **MG 8** 26-39 arXiv: gr-qc/9712070

[5] Goroff M Sagnotti A 1985 Quantum gravity at two loops *Phys.Lett.B* **160** 81-86

[6] Thiemann T 2007 *Modern Canonical Quantum General Relativity* Landshoff Nelson Weinberg (Cambridge: Cambridge University Press)

[7] Martin B Shaw G 2017 *Particle Physics* (Chichester: John Wiley and Sons Ltd)

[8] Major S 1999 A Spin Network Primer *Am.J.Phys.* **67** 972-980

[9] Ashtekar A Singh P 2011 Loop Quantum Cosmology: A Status Report *Class.Quant.Grav.* **28** 213001

[10] Unger G Poplawski N 2019 Big bounce and closed universe from spin and torsion *Astrophys. J.* **870** 2

[11] Ashtekar A Sloan D 2010 Loop quantum cosmology and slow roll inflation *Phys.Lett.B* **694** 108-112

[12] Singh P 2009 Are loop quantum cosmos never singular? *Class.Quant.Grav.* **26** 125005

[13] Bianchi E et. al. 2010 Towards Spinfoam Cosmology *Phys.Rev.D* **82** 084035

[14] Rovelli C Vidotto F 2015 *Covariant Loop Quantum Gravity* (Cambridge: Cambridge University Press)

[15] Bekenstein J 1973 Black Holes and Entropy *Phys.Rev.D* **7** 2333-2346

[16] Hawking S 1975 Particle Creation by Black Holes *Commun.math.Phys.* **43** 199-220

[17] Hawking S 1974 Black hole explosions? *Nature* **248** 30-31

[18] Perez A 2017 Black Holes in Loop Quantum Gravity *Rept.Prog.Phys.* **80** 126901

[19] Ashtekar A et. al. 2018 Quantum extension of the Kruskal spacetime *Phys.Rev.D* **98** 126003

[20] Girelli F et. al. 2012 Loop Quantum Gravity Phenomenology: Linking Loops to Observational Physics *SIGMA* **8** 098

[21] Barrau A et. al. 2017 Astrophysical and cosmological signatures of Loop Quantum Gravity

[22] AsapSCIENCE 2015 The War on Science *YouTube*

[23] Arnowitt R Deser S Misner C 1959 Dynamical Structure and Definition of Energy in General Relativity *Phys.Rev.* **116** 1322-1330

[24] Kroon J Mathematical problems of General Relativity: Lecture 2

[25] Tavakoli Y 2014 Lecture II: Hamiltonian formulation of general relativity

[26] Dirac P 1964 *Lectures on quantum mechanics* (New York: Belfer Graduate School of Science)

[27] Ashtekar A 1986 New Variables for Classical and Quantum Gravity *Phys.Rev.Lett* **57** 2244-2247

[28] Ashtekar A 1987 New Hamiltonian formulation of general relativity *Phys.Rev.D* **36** 1587-1602

[29] Fleischhack C 2012 On Ashtekar's formulation of general relativity *J.Phys.Conf.Ser.* **360** 012022

[30] Barbero J 1995 Real Ashtekar variables for Lorentzian signature space times *Phys.Rev.D* **51** 5507-5510

[31] Immirzi G 1997 Real and complex connections for canonical gravity *Class.Quant.Grav.* **14** L177-L181

[32] Magueijo J Private correspondence

[33] Baez J 2000 An Introduction to spin foam models of quantum gravity and BF theory *Lect.Notes Phys.* **543** 25-94

[34] Nicolai H et. al. 2005 Loop quantum gravity: An Outside view *Class.Quant.Grav.* **22** R193

[35] Smolin L 2004 An Invitation to loop quantum gravity *QTS-3* 655-682 arXiv: hep-th/0408048

[36] Loll R 1994 Gauge theory and gravity in the loop formulation *Canonical Gravity: From Classical to Quantum. Lecture Notes in Physics* **434** 254-288

[37] Rovelli C 1998 Loop quantum gravity *Living Rev.Rel.* **1** arXiv: gr-qc/9710008

[38] Smolin L 1992 Recent developments in nonperturbative quantum gravity *Sant Feliu de Guixols 1991, Proceedings, Quantum gravity and cosmology* 3-84 arXiv: hep-th/9202022

[39] Rovelli C Smolin L 1995 Spin networks and quantum gravity *Phys.Rev.D* **52** 5743-5759

[40] Gambini R Pullin J 1996 *Loops, Knots, Gauge Theories and Quantum Gravity* (Cambridge: Cambridge University Press)

[41] Jacobson T Smolin L 1988 Nonperturbative quantum geometries *Nucl.Phys.B* **299** 295-345

[42] DeWitt B 1967 Quantum Theory of Gravity. I. The Canonical Theory *Phys.Rev* **160** 1113-1148

[43] Perez A 2004 Introduction to loop quantum gravity and spin foams *ICFI 2004* arXiv: gr-qc/0409061

[44] Baez J et. al. 1994 *Knots and Quantum gravity* Baez (Oxford: Clarendon Press)

[45] Thiemann T 1996 Anomaly-free formulation of nonperturbative, four-dimensional Lorentzian quantum gravity *Phys.Lett.B* **380** 257-264

[46] Thiemann T 1998 Quantum Spin Dynamics (QSD) *Class.Quant.Grav.* **15** 839-873

[47] Thiemann T 1998 Quantum Spin Dynamics (QSD) II *Class.Quant.Grav.* **15** 875-905

[48] Thiemann T 2006 The Phoenix project: Master constraint program for loop quantum gravity *Class.Quant.Grav.* **23** 2211-2248

[49] Smolin L 1996 The Classical limit and the form of the Hamiltonian constraint in nonperturbative quantum general relativity arXiv: gr-qc/9609034

[50] Lewandowski J Marolf D 1998 Loop constraints: A Habitat and their algebra *Int.J.Mod.Phys.D* **7** 299-330

[51] Gambini R et. al. 1998 On the consistency of the constraint algebra in spin network quantum gravity *Int.J.Mod.Phys.D* **7** 97-109

[52] Thiemann T 2006 Quantum spin dynamics. VIII. The Master constraint *Class.Quant.Grav.* **23** 2249-2266

[53] Dittrich B Thiemann T 2006 Testing the master constraint programme for loop quantum gravity. V. Interacting field theories *Class.Quant.Grav.* **23** 1143-1162

[54] Mäkinen I 2019 Introduction to SU(2) Recoupling Theory and Graphical Methods for Loop Quantum Gravity arXiv: 1910.06821

[55] Bastin T 1971 *Quantum Theory and Beyond* (Cambridge: Cambridge University Press)

[56] Baez J 1995 Spin networks in nonperturbative quantum gravity *The Interface of Knots and Physics* 167-203 arXiv: gr-qc/9504036

[57] Kauffman L Lins S 1994 *Temperley-Lieb Recoupling Theory and Invariants of 3-Manifolds* (Princeton: Princeton University Press)

[58] De Pietri R Rovelli C 1996 Geometry eigenvalues and scalar product from recoupling theory in loop quantum gravity *Phys.Rev.D* **54** 2664-2690

[59] Baez J 1998 Spin foam models *Class.Quant.Grav.* **15** 1827-1858

[60] Reisenberger M Rovelli C 1997 'Sum over surfaces' form of loop quantum gravity *Phys.Rev.D* **56** 3490-3508

[61] Rovelli C 1999 The Projector on physical states in loop quantum gravity *Phys.Rev.D* **59** 104015

[62] Reisenberger M 1994 World sheet formulations of gauge theories and gravity *MG* **7** arXiv: gr-qc/9412035

[63] Hartle J 1993 The Space-time approach to quantum mechanics *Vistas Astron.* **37** 569

[64] Regge T 1961 General relativity without coordinates *Nuovo Cim* **19** 558–571

[65] Stover C 2020 Regge Calculus

[66] Weisstein E 2020 Simplex

[67] Weisstein E 2020 Skeleton

[68] Ponzano G Regge T 1969 Semiclassical limit of Racah coefficients *Spectroscopic and Group Theoretical Methods in Physics* **F** 1-58

[69] Crane L Yetter D 1993 A Categorical construction of 4-D topological quantum field theories *Dayton 1992, Proceedings, Quantum topology* 120-130 arXiv: hep-th/9301062

[70] Crane L et. al. 1994 State sum invariants of four manifolds. 1. arXiv: hep-th/9409167

[71] Maran S 2003 Construction of the general spin foam model of Lorentzian BF theory and gravity arXiv: gr-qc/0311094

[72] Barrett J Crane L 1998 Relativistic spin networks and quantum gravity *J.Math.Phys.* **39** 3296-3302

[73] Barrett J Crane L 2000 A Lorentzian signature model for quantum general relativity *Class.Quant.Grav.* **17** 3101-3118

[74] Perez A 2003 Spin foam models for quantum gravity *Class.Quant.Grav.* **20** R43

[75] Pietri R Freidel L 1999 so(4) Plebanski action and relativistic spin foam model *Class.Quant.Grav.* **16** 2187-2196

[76] Engle J et. al. 2008 LQG vertex with finite Immirzi parameter *Nucl.Phys.B* **799** 136-149

[77] Engle J et. al. 2007 The loop quantum gravity vertex amplitude *Phys.Rev.Lett.* **99** 161301

[78] Reisenberger M 1999 On relativistic spin network vertices *J.Math.Phys.* **40** 2046-2054

[79] Crane L et. al. 2001 A finiteness proof for the Lorentzian state sum spinfoam model for quantum general relativity arXiv: gr-qc/0104057

[80] Engle J et. al. 2008 Flipped spinfoam vertex and loop gravity *Nucl.Phys.B* **798** 251-290

[81] Pereira R 2007 Lorentzian LQG vertex amplitude *Class.Quant.Grav.* **25** 085013

[82] Mikovic A Vojinovic M 2013 A finiteness bound for the EPRL/FK spin foam model *Class.Quant.Grav.* **30** 035001

[83] Engle J 2012 A spin-foam vertex amplitude with the correct semiclassical limit *Phys.Lett.B* **724** 333-337

[84] Engle J 2011 A proposed proper EPRL vertex amplitude *Phys.Rev.D* **87** 084048

[85] Barrett J et. al. 2010 Lorentzian spin foam amplitudes: graphical calculus and asymptotics *Class.Quant.Grav.* **27** 165009

[86] Oriti D 2006 The Group field theory approach to quantum gravity arXiv: gr-qc/0607032

[87] Polchinski J 1998 *String Theory: Volume I* (Cambridge: Cambridge University Press) Polchinski J 1998 *String Theory: Volume II* (Cambridge: Cambridge University Press)

[88] Ashtekar A et. al. 2000 Quantum geometry of isolated horizons and black hole entropy *Adv.Theor.Math.Phys.* **4** 1-94

[89] Ford I 2013 *Statistical Physics: An Entropic Approach* (Chichester: John Wiley and Sons Ltd)

[90] Unruh W 1976 Notes on Black Hole Evaporation *Phys.Rev.D* **D14** 870-892

[91] Frodden E et. al. 2011 Quasilocal first law for black hole thermodynamics *Phys.Rev.D* **87** 121503

[92] Krasnov K 1998 On Quantum statistical mechanics of Schwarzschild black hole *Gen.Rel.Grav.* **30** 53-68

[93] Ghosh A Perez A 2011 Black hole entropy and isolated horizons thermodynamics *Phys.Rev.Lett.* **107** 241301

[94] Bekenstein J 1974 The quantum mass spectrum of the Kerr black hole *Lettere al Nuovo Cimento* **11** 467-470

[95] Mukhanov V 1986 Are black holes quantized? *ZhETF Pisma Redaktsiiu* **44** 50-53

[96] Bekenstein J Mukhanov V Spectroscopy of the quantum black hole *Phys.Lett.B* **360** 7-12

[97] Barreira M et. al. 1996 Physics with nonperturbative quantum gravity: radiation from a quantum black hole *Gen.Rel.Grav.* **28** 1293-1299

[98] Krasnov K 1999 Quantum geometry and thermal radiation from black holes *Class.Quant.Grav.* **16** 563-578

[99] Gambini R Pullin J 2014 Hawking radiation from a spherical loop quantum gravity black hole *Class.Quant.Grav.* **31** 115003

[100] Barrau A et. al. 2011 Probing Loop Quantum Gravity with Evaporating Black Holes *Phys.Rev.Lett.* **107** 251301

[101] Barrau A et. al. 2015 Black hole spectroscopy from Loop Quantum Gravity models *Phys.Rev.D* **92** 124046

[102] Barrow J 2020 The Area of a Rough Black Hole *Phys.Lett.B* **808** 135643

[103] Koch H 1904 Sur une courbe continue sans tangente, obtenue par une construction géométrique élémentaire *Arkiv för Matematik* **1** 681–704

[104] Hausdorff F 1919 Dimension und äußeres Maß *Math. Ann.* **79** 157-179

[105] Abreu E et. al. 2020 Barrow's black hole entropy and the equipartition theorem *EPL* **130** 40005

[106] Abreu E Neto J 2020 Barrow fractal entropy and the black hole quasinormal modes *Phys.Lett.B* **807** 135602

[107] Abreu E Neto J 2020 Thermal features of Barrow corrected-entropy black hole formulation *EPJ C* **80** 776

[108] Haggard H Rovelli C 2015 Black hole fireworks: quantum-gravity effects outside the horizon spark black to white hole tunneling *Phys. Rev. D* **92** 104020

[109] Ashtekar A et. al. 2018 Quantum Transfiguration of Kruskal Black Holes *Phys.Rev.Lett.* **121** 241301

[110] Ashtekar A Olmedo J 2020 Properties of a recent quantum extension of the Kruskal geometry *Int.J.Mod.Phys.D* **29** 2050076

[111] Faraoni V Giusti B 2020 Unsettling physics in the quantum-corrected Schwarzschild black hole *Symmetry* **12** 1264

[112] Heidmann P et. al. 2017 Semi-classical analysis of black holes in Loop Quantum Gravity: Modelling Hawking radiation with volume fluctuations *Phys.Rev.D* **95** 044015

[113] Bianchi E 2020 Status of the Spinfoam Vertex

[114] Asante S et. al. 2020 Effective Spin Foam Models for Four-Dimensional Quantum Gravity arXiv: 2004.07013

[115] Vaid D 2017 Connecting Loop Quantum Gravity and String Theory via Quantum Geometry arXiv:1711.05693v3

[116] Shoshany B 2020 Spin Networks and Cosmic Strings in 3+1 Dimensions *Class.Quant.Grav.* **37** 085019

[117] Noui K Perez A 2005 Three dimensional loop quantum gravity: physical scalar product and spin foam models *Class.Quant.Grav.* **22** 1739-1762

[118] Sen A 2013 Logarithmic Corrections to Schwarzschild and Other Non-extremal Black Hole Entropy in Different Dimensions *JHEP* **2013** 156

[119] Stack Exchange 2020 Does Loop Quantum Gravity predict general relativity in semi-classical Limit?

[120] Rovelli C Vidotto F 2014 Planck stars *Int.J.Mod.Phys.D* **23** 1442026

[121] Amelino-Camelia G Piran T 2001 Planck-scale deformation of Lorentz symmetry as a solution to the ultra high energy cosmic ray and the TeV-photon paradoxes *Phys.Rev.D* **64** 036005